

Author Version of : *Global Biogeochemical Cycles*, vol.32(3); 2018; 417-436

²³⁴Th based carbon export flux along the Indian GEOTRACES GI02 section in the Arabian Sea and the Indian Ocean

S. Subha Anand¹, R. Rengarajan^{1*}, V.V.S.S. Sarma²

¹Geoscience Division, Physical Research Laboratory, Navrangpura, Ahmedabad, Gujarat, India

²CSIR-National Institute of Oceanography, Regional Centre, Visakhapatnam, Andhra Pradesh, India

*Corresponding Author: R. Rengarajan

E-mail: rajan@prl.res.in, Phone: +91 79 2631 4314

Abstract

²³⁴Th ($t_{1/2} = 24.1$ d), present in seawater, is a naturally occurring particle-reactive radionuclide formed through the radioactive decay of its parent, ²³⁸U ($t_{1/2} = 4.47 \times 10^9$ y). The ²³⁴Th:²³⁸U disequilibrium is exploited to quantify fluxes of elements moving out of the euphotic zone by attaching on to sinking particles. Under the Indian GEOTRACES programme, high-resolution sampling in the upper 300 m depth was carried out at 11 stations in the Arabian Sea and the Indian Ocean during April – May 2014 from 17°N to 16°S along 65°E transect to estimate the ²³⁴Th based particulate organic carbon (POC) export flux from the upper ocean. Average ²³⁴Th fluxes integrated to 100 m depth were 2612 and 1968 dpm m⁻² d⁻¹ for the Arabian Sea and the Indian Ocean, respectively. The estimated POC export fluxes ranged from negligible to 9.0 mmol m⁻² d⁻¹ and the ²³⁴Th based POC export efficiencies were <2 to 5%. For the same season, the Arabian Sea and the Bay of Bengal showed highly contrasting carbon export trends (mean: 4.0 and 0.8 mmol C m⁻² d⁻¹, respectively). The modeled POC export fluxes from in situ and satellite derived primary production are higher than the ²³⁴Th based values for the Laws and Dunne models and are comparable for the Henson model. The modeled POC fluxes which depend on surface temperature and primary production could be further refined for the seasonal cycle in biological productivity and associated differences in trophic structure, grazing intensity, recycling efficiency, high bacterial activity and associated DOC export.

Keywords: ²³⁴Th, POC export flux, GEOTRACES, Biological carbon pump, Indian Ocean, Arabian Sea

Key Points :

1. We present the first ²³⁴Th based POC export flux estimates along the 65°E meridional transect in the Arabian Sea and the Indian Ocean
2. In contrast to episodic decrease of primary production from 17°N to 16°S, ²³⁴Th based POC export fluxes show high values in the Indian Ocean
3. ²³⁴Th deficit in subsurface depths is due to the diel vertical migration, grazing and fecal pellet production by mesozooplankton

1. Introduction

Marine phytoplankton accounts for about half of the world's net primary production of biogenic carbon (Geider et al., 2014). The export of biogenic particles from the euphotic zone to the deep plays a crucial role in the marine carbon cycle. The oceanic biological carbon pump, the conversion of CO₂ into biomass and subsequent sinking from the surface layer through the mesopelagic zone, plays a key role in the global carbon cycle with its export magnitude ranging from 4 to 12 Pg C y⁻¹ (Henson et al., 2011; DeVries and Weber, 2017). Global patterns of POC export revealed high export rate occurring in the high latitude North Atlantic, the Arctic and the Southern Ocean and low particle export efficiency at low latitudes (Le Moigne et al., 2013; Henson et al., 2012). However, sudden export events like the occurrence of phytoplankton blooms enhance POC export flux at all latitudes (Buesseler, 1998a, 1998b; Thomalla et al., 2008).

The Indian Ocean is of great interest to oceanographers as it experiences seasonally reversing monsoon winds and surface ocean currents. The tropical Indian Ocean forms the significant part of the largest warm pool, which is known to have greater impact on the global climate. The Indian Ocean warm pool is not only the site of intra-seasonal variability in the monsoon system but also a region from which global climate signals radiate (Webster et al., 1997). The Indian Ocean encompasses (i) the Arabian Sea, one of the strongest upwelling zones on earth with high seasonally varying primary productivity, (ii) Bay of Bengal which is fresh water stratified and less productive, (iii) the equatorial Indian Ocean which lacks climatological upwelling unlike other two tropical oceans and (iv) the southern Indian Ocean (Kothawale et al., 2007; Vinayachandran and Shetye, 1991; McCreary et al., 2013). In the recent decades, sea surface temperature and heat content of this region have been increasing continuously (Schott et al., 2009). The rising atmospheric CO₂ levels and sea surface temperature might influence the ability of the biological carbon pump to export POC from the euphotic zone (Riebesell et al., 2007).

During 1994–1996, the northern Arabian Sea has been extensively studied, as part of the Joint Global Ocean Flux Study (JGOFS). One of the peculiar properties of the Arabian Sea is the semi-annual reversal of wind regimes caused by the monsoon. These reversals have a significant impact on the upper ocean circulation and biological productivity of the region (Qasim, 1982; Madhupratap et al., 1996; Barber et al., 2001). The negative water balance associated with excess evaporation over precipitation and intrusion from the Mediterranean Sea makes the Arabian Sea high saline (>36). Some of the biogenic particles produced in surface water settle to the interior where these are remineralised. These biogeochemical processes coupled with restricted ventilation contribute to

extreme depletion of oxygen in the intermediate waters (100–1200 m depth). This generates a widespread oxygen minimum zone (OMZ) with active denitrification (Naqvi, 1991, 1994) in the intermediate waters.

The Indian Ocean is important for the study of the global biological carbon pump and how high resolution global biogeochemical models succeed at capturing POC export for areas of the ocean with seasonal variability, upwelling, and oxygen minimum zones. Measuring the POC export flux can be accomplished by directly collecting material that sinks into sediment traps (Honjo, 1996) or by using tracers with well-constrained radionuclide production in surface waters (Cochran, 1992). To estimate POC export flux, the ^{234}Th ($t_{1/2} = 24.1$ d) based approach is considered advantageous as the technique determines the downward flux of ^{234}Th from a single water column profile of ^{234}Th and the $\text{POC}/^{234}\text{Th}$ ratio in sinking particulate matter, thus avoiding complications associated with sediment trap deployments (Buesseler et al., 1992). The global database of ^{234}Th based POC export flux contains data collected from the equatorial Pacific, North Atlantic, South China Sea and the Arabian Sea with no representative data for the western Pacific, Mauritian upwelling and the equatorial and southern Indian Ocean (Le Moigne et al., 2013). Our knowledge on ^{234}Th based POC export in the Indian Ocean is limited to the estimates made two decades earlier by Sarin et al. (1994 and 1996) and Buesseler et al. (1998a) in the Arabian Sea as a part of JGOFS programme and a recent study by Anand et al. (2017) along 87°E transect in the Bay of Bengal and the Indian Ocean. In the present study, we report vertical profiles of total ^{234}Th and ^{238}U concentrations and $^{234}\text{Th}/^{238}\text{U}$ activity ratios in the upper 300 m and estimate the upper ocean POC export flux along 65°E transect in the Arabian Sea and the Indian Ocean during spring intermonsoon (April-May 2014). The primary goals of this study are (1) to determine the spatial variability of POC export flux in the Arabian Sea and the Indian Ocean along 65°E transect (2) to understand the role of subsurface chlorophyll maxima in carbon export and impact of bacterial production, zooplankton grazing and sinking of fecal pellets on ^{234}Th distribution at sub-surface waters (3) to compare ^{234}Th based POC export flux in the Arabian Sea and the adjacent basin –the Bay of Bengal during the same season and (4) to compare measured and modeled primary production and POC export fluxes.

2. Methods

2.1. Sampling

Seawater samples for total ^{234}Th were collected during April – May 2014 onboard the ORV SagarKanya (Cruise No. SK312, GEOTRACES GI02 section) and covered a wide range of settings from the low productive southern Indian Ocean (16°S) through the oligotrophic equatorial Indian

Ocean to the Arabian Sea (17°N) along 65°E transect. Sampling took place from Port Louis, Mauritius (27 April 2014) to Mormugao port, Goa (30 May 2014) (Figure 1). Water column profiles for total ^{234}Th were collected from surface to 300 m depth at 11 stations at ~ 3 to 4° intervals along the cruise track. These include 5 stations from the Arabian Sea, 3 from the oligotrophic equatorial Indian Ocean and 3 from the low-productive southern Indian Ocean. Complete details on exact station location, sampling date, total water column depth, sampling depths are given in Table 1.

2.2. ^{234}Th derived POC export fluxes and POC export efficiency

At each station, seawater samples for total ^{234}Th were collected from 11 depths (0-300 m) by using Niskin samplers attached to clean, trace metal free CTD rosette system. The samples were immediately sub-sampled into 4 L Nalgene bottles and processed for total ^{234}Th on board by following the procedures of Buesseler et al. (2001), Cai et al. (2006b) and Anand et al. (2017). In brief, the seawater samples were acidified and spiked with 250 μL of ^{230}Th tracer (30.7 ± 0.9 dpm mL^{-1}) and allowed to equilibrate. After equilibration, pH of the samples was raised to ~ 8.2 and precipitated using KMnO_4 and MnCl_2 . The MnO_2 precipitate was filtered on a 25 mm QMA filter (1 μm nominal pore size) and dried in a hot air oven. The filtrate was then mounted, packed and counted immediately on a RISØ anticoincidence, low background beta counting system (DTU Nutech, Denmark) installed onboard to measure the initial counts of ^{234}Th from beta emission of ^{234}Pa [$E_{\text{max}} = 2.19$ MeV]. To test the performance and efficiency of the detectors, ^{99}Tc high activity standards (supplied with the counters) were counted onboard at the start and end of the cruise. Identical standards were counted in all the five detectors to check the variability in efficiency between the detectors. Six months later, after recording the background counts, the samples were demounted and prepared for ^{230}Th percent recovery and ^{234}Th chemical yield in the MnO_2 precipitate. Towards this, the MnO_2 precipitate was dissolved, spiked with ~ 700 mg of ^{229}Th tracer (108.19 pg g^{-1} or 51.074 dpm g^{-1}) and equilibrated. Column chemistry was performed to purify Th from other elements and the final solution was prepared in 0.4 M HNO_3 . Ratio of $^{229}\text{Th}/^{230}\text{Th}$ was determined by using XSERIES 2 Quadrupole ICP-MS (Thermo Scientific, Germany). Average recoveries of $92.2 \pm 8.5\%$ were obtained ($n = 102$). Measurements of seawater samples at 2000 m depth (Table 1) showed an average $^{234}\text{Th}/^{238}\text{U}$ A.R. of 1.03 ± 0.03 ($n=2$). ^{238}U was estimated from salinity by following the salinity-uranium relationship given by Pates and Muir (2007) and Owens et al. (2011). Uranium concentration and $^{234}\text{U}/^{238}\text{U}$ isotopic composition of seawater collected from oxic and sub-oxic regions of the Arabian Sea showed that, in general, uranium behaves conservatively in these regions (Rengarajan et al., 2003). Their results showed that anoxic respiration

(denitrification) did not remove detectable amounts of uranium from the intermediate waters of the Arabian Sea and that the biogeochemical processes associated with denitrification did not influence, to any measurable levels, the water column geochemistry of uranium in these waters.

For particulate ^{234}Th measurement, 8 L of seawater sample collected from 200 m depth was filtered immediately onto a pre-combusted QMA filter (1 μm nominal pore size) without any processing and dried and mounted on clean plastic holder prior to counting on a beta counter. Six months later, after recording the background counts, the samples were exposed to acid fumes to remove inorganic carbon and POC was measured using a Flash 2000 Organic Elemental CN analyzer (Thermo Fischer Scientific, UK). Before measurement, the analyzer was calibrated using Low Organic Soil Sample (LOSS) containing 1.65% carbon as standards selected within the samples' range. Measurement precision of total carbon is determined by repeated measurements of LOSS standards and was found to be $\pm 3\%$. The C blank of the dipped filter was generally $<10\%$ of the POC on the QMA filters. No correction was made for possible adsorption of ^{234}Th on the QMA filters (Moran et al., 1999; Benitez-Nelson et al., 2001; Buesseler et al., 2006; Rutgers van der Loeff et al., 2006). For particulate ^{234}Th measurement, we kept the filtration time short so that seawater contact time with the QMA filter was minimal. Thus adsorption of dissolved ^{234}Th on to QMA filter was minor during our sampling period.

In previous studies, bottle POC/ ^{234}Th ratios were consistently higher than for large particles collected using large volume in situ pumps (Liu et al., 2005; Chen, 2008). It is suggested that the elevated POC/ ^{234}Th ratio on particles for bottle filtration may be caused by dissolved organic carbon adsorption and /or preferential capture of living zooplankton with elevated POC/ ^{234}Th ratios (Buesseler et al., 2006; Cai et al., 2008; Liu et al., 2009). In a recent study, Zhou et al. (2016) observed that the effect of adsorption on the POC/ ^{234}Th ratio on particles collected by both bottles and pumps would be negligible since the adsorption-corrected and –uncorrected POC/ ^{234}Th ratios were similar. The positive offset in POC/ ^{234}Th ratios between bottle and pump sampling can be caused by zooplankton invasion and/or artificial particle formation. The adsorption effect might not have been large enough to elevate bottle POC/ ^{234}Th ratios as reported earlier. In this study, major discrepancies in POC measurements like adsorption of DOC onto filter, small sample volume ($\sim 1\text{-}2$ L) and capture of live zooplankton inside Niskin sample bottles were avoided by filtering 8 L seawater onto 25 mm QMA filter (Cai et al., 2008).

In general, the POC/ ^{234}Th ratio in sinking particles steadily decreased with depth which is believed to be caused by preferential remineralization of organic carbon (Buesseler et al., 2006). In addition, Cai

et al. (2006a, 2015) and Black et al. (2017) noted that the size-fractionated POC/²³⁴Th ratio showed greater variation at the surface than below the euphotic zone and became roughly invariant at 100–200 m depth. Puigcorbé et al. (2015) showed using high resolution in situ pump sampling that POC/²³⁴Th ratios in large and small particles converged with increasing depth and were comparable at 100 – 500 m depth. Thus, use of POC/²³⁴Th ratio on particles below euphotic zone will not cause significant error in the calculation of POC export flux. There are several studies on variability of POC fluxes and the factors controlling the POC/²³⁴Th ratio in suspended and sinking particles as well as its dependency on the size and biochemical processes (Hung et al., 2004; Buesseler et al., 2006; Xu et al., 2011; Wei et al., 2011). For example, based on a sediment trap study in the northwest Pacific Ocean, Hung et al. (2012) demonstrated that sinking particles contained abundant diatom cells, fecal pellets, detritus and small particle aggregates mostly < 50 µm that can account for a major fraction of the bulk sinking particles in open ocean regions and ²³⁴Th was mainly carried by the smaller (<50 µm) sinking particles. A study by Sarma et al. (2016) suggested that stratification in the Bay of Bengal significantly influenced both (1) the input of nutrients to the sunlit zone, resulting in differences in phytoplankton biomass, and (2) size structure in the picoplankton dominating the phytoplankton population in the Bay due to limited supply of nutrients and low nutrient requirements. Similarly in the Arabian Sea, the incoming short-wave radiation was maximum during spring intermonsoon. The intense solar heating resulted in the highly stratified and shallow mixed layer. The weak winds prevalent during this time of the year were unable to break the stratification and induce mixing of subsurface waters with surface waters. As a result, the upper layer was devoid of any nutrients resulting in oligotrophic mixed layer (Kumar and Narvekar, 2005). Morrison et al. (1998) reported very low nutrient levels (below detection levels) in the southern Arabian Sea during spring intermonsoon and hypothesized that the planktonic system retains nutrients via local recycling processes. Ramaiah et al. (1996) reported that the Arabian Sea was dominated by picoplankton during February–March and by bacteria during April–May. Richardson and Jackson (2007) suggested that aggregation of picoplankton cells into larger detrital particles and mesozooplankton grazing enhanced sinking of smaller particles and their export from the surface layer of the ocean in the Arabian Sea. Puigcorbé et al. (2015) compiled global POC/²³⁴Th data and found that the POC/²³⁴Th ratios do not increase with increasing particle size when pico- and nanoplankton dominate the phytoplankton community. They also reported that the POC/²³⁴Th ratios in small particles collected at 100 m were in better agreement with sediment trap ratios than those of large particles. Thus, the particles were collected in this study only at 200 m using 1 µm QMA filters which are justified

within the estimated uncertainty in representing potentially sinking material to the vertical ^{234}Th and POC export flux.

According to the half-lives of the parent and daughter nuclides, ^{238}U and ^{234}Th are expected to be in secular equilibrium with each other. However, the downward flux of particles removes ^{234}Th and breaks the equilibrium. The ^{234}Th flux scavenged from the upper ocean is estimated from the general equation:

$$\frac{\partial \text{Th}}{\partial t} = \lambda_{234}(A_{238} - A_{234}) - P + V \quad (1)$$

where, $\frac{\partial \text{Th}}{\partial t}$ is the change of total ^{234}Th activity with time, A_{234} is the measured activity of total ^{234}Th in dpm L^{-1} , A_{238} is the activity of ^{238}U (generally derived from measured salinity), λ_{234} is the decay constant of ^{234}Th (0.02876 d^{-1}), P is the scavenging rate of ^{234}Th by particles ($\text{dpm L}^{-1} \text{ d}^{-1}$), V is the sum of advection and diffusion terms. This model assumes a steady state that both the activities and fluxes are assumed to be constant for time scales shorter than 35 d (mean-life of ^{234}Th). Winds over the Arabian Sea were weakest in the intermonsoon months of April and October from drifter and satellite data averaged over several years (Beal et al., 2013). When averaged over 0-100 m and the mean life of ^{234}Th , the modeled horizontal velocities were small, $< 10 \text{ cm s}^{-1}$, but ADCP based upper ocean maximum current speed (measured at 21 m depth) ranged from 50 to 80 cm s^{-1} which is comparatively lower than that during the Southwest Monsoon ($\sim 150 \text{ cm s}^{-1}$) (Flagg and Kim, 1998). Buesseler et al. (1998a) estimated ^{234}Th based POC export fluxes in the Arabian Sea during spring intermonsoon (March-April 1995) and showed those were similar for both steady-state and non-steady-state models. In view of the above evidences, steady-state assumptions may be reasonable.

The ^{234}Th flux (F_{Th}) integrated to depth, z is proportional to the disequilibrium between ^{234}Th and ^{238}U and is calculated by assuming a closed system at steady state as

$$F_{Th} = \lambda_{234} \int_0^z (A_{238} - A_{234}) dz \quad (2)$$

The ^{234}Th based POC export fluxes were derived from ^{234}Th : ^{238}U disequilibrium, by multiplying ^{234}Th flux scavenged from the upper ocean with the POC/ ^{234}Th ratio measured in particulate matter filtered at 200 m depth. POC export efficiency is defined as the ratio of estimated ^{234}Th based POC flux sinking through the euphotic zone to primary production. This is considered as a measure of the strength of the biological pump.

2.3. Insitu primary production and satellite based primary production

The primary production was estimated by following the methods of Hama et al. (1983) and elaborated in Anand et al. (2017). In brief, primary production in the euphotic zone of the seawater column was measured using enriched sodium bicarbonate ($\text{NaH}^{13}\text{CO}_3$). About 1 L seawater samples were collected at each depth in the photic zone and incubated with enriched sodium bicarbonate. Samples were incubated on deck under controlled light and temperature conditions for 24 hours and filtered onto precombusted GF/F filters. The samples were measured for POC concentration and isotopic composition of carbon and nitrogen using isotope ratio mass spectrometer (IRMS; Delta V Plus, Thermo Electron, Germany) further converted to primary production following Hama et al. (1983).

To compare the insitu primary production with satellite based net primary productivity estimates, NPP data were obtained from the Oregon state university ocean productivity webpage (<http://www.science.oregonstate.edu/ocean.productivity/>). NPP data were downloaded for the two widely used primary productivity models-vertically generalized productivity model (VGPM) and carbon-based productivity model (CbPM) and mean NPP calculated for each station by defining a squared region of 0.5° surrounding the station (Roullier et al., 2014).

3. Results

3.1. Hydrography

Vertical profiles of salinity, temperature, density structure and oxygen saturation (%) along the 65°E meridional section of the Arabian Sea and the Indian Ocean are shown as white contour lines relative to DIN, phosphate, silicate and fluorescence, respectively, in Figures 2a-d. The figures reveal the occurrence of high salinity water (36.641) in the northern Arabian Sea between 17°N and 13°N while salinity contours showed subsurface shoaling towards south of equator. Sea surface temperature was high ($30\text{-}31^\circ\text{C}$) in the Arabian Sea and decreased towards the south of equator (27°C at 16°S). Upheaving of isotherms at the subsurface depths was observed to the north and south of equator. The density gradients (σ_θ) were strong (range: 21 – 27) and well correlated with depth of nutricline. The relation between potential temperature and salinity during the spring intermonsoon (Figure 3) indicated the presence of different water masses in the surface and subsurface depths of the northern Arabian Sea. The structure of the upper layers of the Arabian Sea is dictated by the transport and mixing of the Arabian Sea high salinity water (ASHW, $\sigma_\theta = 22.8\text{-}24.5$), Persian Gulf water (PGW,

$\sigma_\theta = 26.2\text{--}26.8$) and the Red Sea water (RSW, $\sigma_\theta = 27.0\text{--}27.4$) (Shetye et al., 1994; Kumar and Prasad, 1999).

Saturation to supersaturation of oxygen was observed in the upper 50 m of the water column and decreased to 40-80% at the depth below (75 m to 150 m) and then reduced to near zero levels. Dissolved inorganic nitrogen (DIN) concentration was very low in the upper 50 m of water column, along the 65°E transect. However, DIN concentrations increased from 2 to 20 μM between 50 and 100 m depth. Highest concentrations were found below 200 m depth, at stations between 10°N and 10°S. Dissolved inorganic phosphate in the upper 50 m of water column was low ($< 1 \mu\text{M}$). The depth of phosphocline was deeper in the Arabian Sea (~100 m) and shallow in the equatorial region (10°N–10°S; ~75m) and deepened to >200 m in the south Indian Ocean (Figure 2). Low silicate waters ($<2 \mu\text{M}$) were found in the upper 100 m in the Arabian Sea and higher concentrations were observed at 10°S. The depth of silicicline followed phosphocline. Silicate concentrations were high ($> 25 \mu\text{M}$) in the subsurface depths (200-300 m) along the entire transect. Chlorophyll-a (derived from fluorescence) was low in the upper 25 m of water column and prominent subsurface chlorophyll maximum (SCM) was observed in the entire study region. Higher concentrations of SCM was observed at 13°N and 12°S at ~60m. The DCM relatively deeper at the equator compared to either side along the 65°E transect.

3.2. Total ^{234}Th , ^{238}U and $^{234}\text{Th}/^{238}\text{U}$ activity ratio

The total ^{234}Th measured in samples collected between surface and 300 m depth from 11 stations during the cruise varied from 0.98 ± 0.05 to 3.09 ± 0.08 dpm L^{-1} (Table 1). The ^{238}U values varied from 2.40 ± 0.07 to 2.61 ± 0.08 dpm L^{-1} with the highest and lowest activity values being associated with the surface waters. The $^{234}\text{Th}/^{238}\text{U}$ activity ratio was high in the Indian Ocean (1.24 ± 0.05 at 16°S) and low in the Arabian Sea (0.381 ± 0.02 at 16°N). All the stations sampled in the study showed continuous deficit for ^{234}Th relative to ^{238}U , in the sunlit euphotic zone (Figures 4 and 5), except at Sta. 8 (16°S 65°E) that recorded continuous ^{234}Th maxima from surface to 300 m depth. Sta. 17 located at 16°N 65°E in the Arabian Sea recorded highest deficits for ^{234}Th with ^{234}Th values decreasing as low as 0.98 ± 0.05 dpm L^{-1} (Figures 4 and 5). Similar ^{234}Th deficits up to 300 m were reported by Sarin et al. (1996) and are typical for the Arabian Sea. In general, primary production by phytoplankton present in the euphotic zone creates a deficit of ^{234}Th with respect to ^{238}U . However, below the euphotic depth, ^{234}Th remains in equilibrium with ^{238}U or is found in excess in the subsurface depths due to remineralization of organic matter and release of ^{234}Th . In contrast, the stations sampled in the Arabian Sea and the Indian Ocean showed pronounced deficit of ^{234}Th in the

euphotic zone along with subsequent deficit of ^{234}Th in the subsurface depths (150-300 m) (Figure 4). The highest subsurface ^{234}Th deficit was found at Sta. 18, where ^{234}Th value reduced to 1.52 ± 0.05 dpm L^{-1} at 300 m depth.

3.3. Primary Production, POC, Particulate ^{234}Th , POC/ ^{234}Th ratio and Integrated ^{234}Th and POC fluxes

Primary production in all the stations sampled in the study showed an increasing trend from south to north along the 65°E transect and varied by a factor of 3 from 58 ± 3 mmol $\text{C m}^{-2} \text{d}^{-1}$ at 16°S to 179 ± 9 mmol $\text{C m}^{-2} \text{d}^{-1}$ at 17.3°N (Table 2; Figure 6). POC concentration measured at 200 m depth varied from 0.40 to 1.27 μM . Particulate ^{234}Th ranged between 0.210 ± 0.015 and 1.09 ± 0.026 dpm L^{-1} ; whereas the POC/ ^{234}Th ratio ranged from 0.91 ± 0.04 to 3.77 ± 0.29 $\mu\text{mol dpm}^{-1}$. The ^{234}Th fluxes integrated to 100 m depth varied from 1424 ± 90 dpm $\text{m}^{-2} \text{d}^{-1}$ to 2980 ± 87 dpm $\text{m}^{-2} \text{d}^{-1}$ with high fluxes in the Arabian Sea. The average ^{234}Th fluxes in the Arabian Sea were high (2612 ± 88 dpm $\text{m}^{-2} \text{d}^{-1}$) (Sta. 14-18) and were low in the equatorial Indian Ocean (1965 ± 88 dpm $\text{m}^{-2} \text{d}^{-1}$) (Sta. 11-13) (Figure 6). These values are ~5 times higher than those observed on a similar transect along 87°E in the Bay of Bengal (594 dpm $\text{m}^{-2} \text{d}^{-1}$) and the Indian Ocean (539 dpm $\text{m}^{-2} \text{d}^{-1}$) during spring intermonsoon (Anand et al., 2017). The ^{234}Th based POC export fluxes estimated at 100 m depth from ^{234}Th deficit fluxes and POC/ ^{234}Th ratio on particulates collected on 1 μm QMA filter at 200 m depth in the study region varied from negligible to 9.0 ± 0.8 mmol $\text{C m}^{-2} \text{d}^{-1}$.

4. Discussion

4.1. POC export fluxes

The Arabian Sea is known to be oligotrophic during spring intermonsoon season, characterized by low primary production and POC export flux (Latasa and Bidigare, 1998). The single largest feature in the present study is the episodic north-south decrease in primary production (Figure 6). During spring intermonsoon, we find that there exists a significant POC export below the euphotic zone in the Arabian Sea. Although the dissolved nutrient levels were very low in the euphotic zone of the Arabian Sea, the primary production of the basin is comparatively more than that of the Indian Ocean (Figure 2 and 6). Sawant and Madhupratap (1996) reported that the phytoplankton abundance in the central Arabian Sea was quite low during the spring intermonsoon period. Those were mostly related with subsurface chlorophyll maxima and nutricline layers. Autotrophic picoplankton dominate primary production in the Arabian Sea during spring intermonsoon (Latasa and Bidigare, 1998) and believed to contribute less to carbon export from surface layers because of their small

sizes, slow sinking rates and rapid utilization in the microbial loop. However, Richardson and Jackson (2007) suggested picoplankton might contribute more organic carbon export by aggregation of picoplankton cells into larger detrital particles, mesozooplankton grazing and direct feeding by salps.

The POC isotopic composition ($\delta^{13}\text{C}_{\text{POC}}$) varied between -23.4 and -22.1 ‰ in the Arabian Sea suggesting that in situ plankton contributed to POC pool in the study region. The PON isotopic composition ($\delta^{15}\text{N}_{\text{PON}}$) ranged between 5.1 and 10.5 ‰ suggesting that nutrients supplied through in situ processes to support phytoplankton production in the study region. The net community production suggests dominant heterotrophy in the study region due to weak nutrients supply from the subsurface layer to the euphotic zone. In the Arabian Sea during spring intermonsoon higher abundance of total bacteria (Ramaiah et al. 1996) associated with high microzooplankton abundance (Gauns et al., 2005) was observed. Sarma et al. (2003) suggested that active microbial loop supports heterotrophic carbon demand. Thus, low nutrient supply to the euphotic zone triggered microbial loop in the study region that contributed to low POC flux to depth during spring intermonsoon. This is consistent with the earlier observation by Honjo et al. (1998).

Normally bacterial production is ~20% of the primary production. In the central Arabian Sea, biological production was dominated by bacteria during spring intermonsoon, phytoplankton production often accounting for only 2% of the biological production. This suggested the presence of more DOC with the predominance of a microbial loop in food web in this area during spring intermonsoon (Ramaiah et al., 1996; Latasa and Bidigare, 1998). Such high bacterial populations provide evidence for flagellate and ciliate grazing during this season and sustain the zooplankton population in the Arabian Sea (Gauns et al., 1996). Measurement of ΣCO_2 made by Sarma et al. (1996) also supported the intense bacterial activity in the intermediate depths of the Arabian Sea during spring intermonsoon.

The observed deficit of ^{234}Th in the subsurface depths (150-300 m) in the Arabian Sea and the Indian Ocean suggests that there exist a strong grazing and fecal pellet production by mesozooplankton. Relative to other ocean basins, the grazing impact of mesozooplankton is significant in the Arabian Sea. Wishner et al. (1998) studied mesozooplankton biomass distributions in the upper 1000 m of the Arabian Sea in the Spring Intermonsoon and reported that most of the zooplankton biomass occurred in the upper 200 m but there was substantial diel vertical migration, down to 300 - 400 m, well within the suboxic water of the oxygen minimum zone. Roman et al. (2000) estimated total carbon (phytoplankton, protozoa and detritus) ingestion in the surface 200 m in the Northern Arabian

Sea (Average: $44 \text{ mmol C m}^{-2} \text{ d}^{-1}$) and derived zooplankton fecal pellet production (Average: $13 \text{ mmol C m}^{-2} \text{ d}^{-1}$) from the estimated ingestion rates and a 70% assimilation efficiency. Zooplankton exerts a strong grazing pressure on phytoplankton, leaving a small fraction of phytoplankton available for direct export, diminishing the likelihood of algal blooms (Olli et al., 2007). The estimated zooplankton fecal pellet production was greater than the measurements of export flux during spring intermonsoon suggesting that the impact of mesozooplankton grazing was significant in the Arabian Sea due to high zooplankton biomass, abundance of diatoms and warm temperatures (Roman et al., 2000). The potential fecal pellet production is higher by a factor of ~ 3 to the ^{234}Th based POC export flux at 100 m estimated in this study. When estimated fecal pellet production rates are higher than measured export rates, it suggests that fecal pellets are recycled in the upper water column. Similar observations were reported for spring intermonsoon by Roman et al. (2000).

POC export flux estimated using ^{234}Th deficit in the subsurface depths (100-200 m) and POC/ ^{234}Th ratio in particulate matter at 200 m depth, during spring intermonsoon in the Arabian Sea and the Indian Ocean ranged between 0.5 and $6.3 \text{ mmol C m}^{-2} \text{ d}^{-1}$ (mean: $2.4 \pm 2.2 \text{ mmol C m}^{-2} \text{ d}^{-1}$). Wishner et al. (1998) reported that the zooplankton production of $13 \text{ mmol C m}^{-2} \text{ d}^{-1}$ during spring intermonsoon in the Arabian Sea. This is higher by a factor of ~ 5 as compared to the average ^{234}Th based POC export at 100-200 m depth estimated in this study. The estimated fecal pellet production rate ($13 \text{ mmol C m}^{-2} \text{ d}^{-1}$) in the Arabian Sea as reported by Roman et al. (2000) was greater than measurements of export flux at intermediate depths (100-200 m) by a factor of 5. The POC/ ^{234}Th ratio in fresh zooplankton from the northwest Mediterranean were > 100 while the fecal material from these same zooplankton had POC/ ^{234}Th ratios one to three orders of magnitude lower (Rodriguez y Baena et al., 2007). This can be explained by a low surface: volume ratio for zooplankton (enriches POC over ^{234}Th) and decreases in POC/ ^{234}Th ratio with POC assimilation by heterotrophic activity and fecal pellet production (Buesseler et al., 2009). Sarin et al. (1996) reported sediment trap based POC/ ^{234}Th ratio of 20-43 $\mu\text{mol dpm}^{-1}$ at 100-130 m depth during spring intermonsoon in the central Arabian Sea.

Sarin et al. (1994) measured the activities of ^{234}Th and ^{238}U at a few stations along 65°E in the central Arabian Sea and west coast of India during winter monsoon (December 1988) and observed a continuous deficit of ^{234}Th with respect to ^{238}U in the upper 300 m depth of the water column. Additionally, the authors explained that the ^{234}Th deficit remained unaltered in the sub-oxic layers indicating that the oxygen depletion and denitrification processes do not significantly affect the ^{234}Th removal by particles. These continuous ^{234}Th deficit trends from surface to 300 m depth are similar

to those observed in the present study (Table 3). In a similar study made by Sarin et al. (1996) during spring intermonsoon (April-May 1994) in the Arabian Sea, the ^{234}Th export fluxes showed an increasing trend from south ($1345 \text{ dpm m}^{-2} \text{ d}^{-1}$ at 11°N) towards northern Arabian Sea ($1685 \text{ dpm m}^{-2} \text{ d}^{-1}$ at 21.5°N). Results suggest that the POC export flux is substantially higher than primary production indicating the prevalence of an active microbial loop present during this season. Such increasing trends in ^{234}Th export flux was also observed in the present study from $2545 \pm 87 \text{ dpm m}^{-2} \text{ d}^{-1}$ at 10°N to $2980 \pm 87 \text{ dpm m}^{-2} \text{ d}^{-1}$ at 17.3°N . Sarin et al. (1996) estimated high POC export fluxes due to sediment trap based POC/ ^{234}Th ratio ($20 \mu\text{mol dpm}^{-1}$), which is higher than our measured ratios (range: $0.91 - 3.77 \mu\text{mol dpm}^{-1}$). Seasonal studies made by Buesseler et al. (1998a) showed steeper gradients in ^{234}Th flux from the coast of Oman to the central and southern Arabian Sea and the ^{234}Th flux measured across the basin varied between 0 and $> 5000 \text{ dpm m}^{-2} \text{ d}^{-1}$ with low flux during spring intermonsoon in the offshore stations. Our average POC/ ^{234}Th ratio of $2 \mu\text{mol dpm}^{-1}$ is comparable with the ratio reported earlier (range: $2 - 5 \mu\text{mol dpm}^{-1}$) and the estimated average POC export flux of $3.8 \text{ mmol m}^{-2} \text{ d}^{-1}$ in the Arabian Sea is similar to those reported earlier in the central Arabian Sea (range: $0.3 - 2.9 \text{ mmol m}^{-2} \text{ d}^{-1}$) (Buesseler et al., 1998a). Overall, the organic carbon export flux in the Arabian Sea during spring-intermonsoon was found to be low compared to monsoon (Buesseler et al., 1998a). Results of organic carbon measured from shallow sediment traps deployed at $\sim 900 \text{ m}$ water depth in the western Arabian Sea ($16^\circ 20'\text{N } 60^\circ 18.8'\text{E}$) also showed low organic carbon flux $\sim 0.83 \text{ mmol m}^{-2} \text{ d}^{-1}$ (Mohan et al., 2006). A possible mechanism for such reduced export flux, though remineralization at this trap depth is significant, could be due to lack of diatom group of phytoplankton in this season, which could be able to ballast to deeper depth, caused by occurrence of nutrient poor oligotrophic conditions in the photic zone (Gauns et al., 2005).

POC export efficiencies calculated from ^{234}Th based POC export flux to primary production ratio during spring intermonsoon for all the stations in the Arabian Sea and the Indian Ocean were varied between <2 and 7% (Table 2; Figure 6). These values are comparable to the global estimates ($<2-10\%$) derived from surface primary production and POC export flux (Buesseler, 1998b). In a recent study, Anand et al. (2017) reported in situ primary production (range: $13.2 - 173.8 \text{ mmol C m}^{-2} \text{ d}^{-1}$) and POC export flux (range: negligible to $7.7 \text{ mmol C m}^{-2} \text{ d}^{-1}$) for the stations along 87°E transect in the Bay of Bengal and the Indian Ocean during spring intermonsoon period (March – April 2014). For the same season, the Arabian Sea and the Bay of Bengal showed highly contrasting carbon export trends (mean: 4.0 and $0.8 \text{ mmol C m}^{-2} \text{ d}^{-1}$, respectively). Remineralization of organic carbon in the surface and sub-surface waters considerably reduced organic carbon export in the Bay of

Bengal besides annually recurring anticyclonic eddies enhanced organic carbon utilization and heterotrophy.

4.2. Comparison of ^{234}Th based carbon export with modeled flux estimates

There are three empirical models to estimate POC export flux using in situ and/or satellite-derived temperature and net primary production or chlorophyll (Laws, 2000; Laws et al., 2011; Dunne et al., 2005; Henson et al., 2011). These models rely on database of in situ measurements which are sparsely distributed in the oceans both spatially and temporally. Laws (2000) and Laws et al. (2011) developed an empirical relation as a function of PP and surface temperature, T to estimate POC export flux, EF as below:

$$EF_{Laws} = PP \times 0.04756 \times \left(0.78 - \frac{0.43 \times T}{30}\right) \times PP^{0.307} \quad (3)$$

Dunne et al. (2005) derived an empirical equation to predict POC export flux as a function of temperature, euphotic depth and primary production:

$$EF_{Dunne} = PP \times \left\{-0.0101 \text{ } ^\circ\text{C}^{-1} \times T + 0.0582 \times \ln\left(\frac{PP}{Z_{eu}}\right) + 0.419\right\} \quad (4)$$

Henson et al. (2011) got an exponential function using global dataset of only ^{234}Th and trap based export measurements and sea surface temperature:

$$EF_{Henson} = PP \times 0.23e^{-0.08 \times T} \quad (5)$$

We used in situ and satellite based primary production (PP) and surface temperature (T) to calculate POC export flux estimates from the above three models (Table 4). Here 10 m below the deep chlorophyll maximum (DCM) is taken for the depth of euphotic zone (Z_{eu}) (Haskell II et al., 2015). The 1% PAR light level depth was deepest during the sampling period and varied from 80 to 100 m depth (Dickey et al., 1998). Earlier studies in the central Arabian Sea have reported DCM was located at a depth of ~70 m (Bhattathiri et al., 1996; Latasa and Bidigare, 1998). In the absence of PAR measurements, use of DCM+10 m as euphotic depth is justified for the late spring intermonsoon.

The comparison of observed carbon export fluxes and modeled POC fluxes predicted by Henson et al. (2011) are nearly similar while the fluxes predicted by Laws (2000) and Laws et al. (2011) and Dunne et al. (2005) are 2-5 times higher. Earlier comparison made on a global scale showed that in situ export fluxes are lower than that predicted by Laws export model for the temperature range of 20-25°C (Maiti et al., 2016) while, in the present study, the maximum SST is extended upto 31°C.

Although all the models showed significant carbon export, at Sta. 8 (16°S 65°E), there is no ^{234}Th based POC export. The excess ^{234}Th than ^{238}U observed in the upper water column restrict the ability of the model to predict fluxes at this station.

Overall, we find the average in situ primary production to be higher, by a factor of 3 – 6, than the VGPM and CbPM primary production estimates. However, the CbPM primary production estimates in the study area are 127% higher compared to the VGPM estimates (Figure 7). The reason for such difference is beyond the scope of the present study, so we have used both in situ primary production and VGPM, CbPM values for comparison. The ^{234}Th based POC export flux is similar to the estimates from Henson model while Laws and Dunne models show comparatively higher export flux in the study region. A plot showing relation between POC export fluxes estimated from ^{234}Th flux and various models, and in situ primary production is shown in Figure 8. The model based POC export flux increases with increasing primary productivity for the Laws (3-15 $\text{mmol m}^{-2} \text{d}^{-1}$) and Dunne model (5-30 $\text{mmol m}^{-2} \text{d}^{-1}$) (Figure 8). However, the Henson model does not show any significant increase though primary production increased from 58 to 180 $\text{mmol m}^{-2} \text{d}^{-1}$. The ^{234}Th derived flux based export efficiencies vary from 0.014 - 0.070 and the model based export efficiencies vary around 0.02 for Henson model, 0.13 - 0.17 and 0.091 - 0.184 for the Laws and Dunne models. The POC export efficiency values are similar to export efficiencies derived from the Henson model whereas these are higher for the Laws and Dunne models (Figure 9). Although the observed export fluxes and export efficiencies between in situ measurements and the Henson model are comparable, this model does not seem to represent the variations observed in the ^{234}Th based fluxes.

On a global scale, the Henson model could be applied to predict export fluxes and export efficiencies whereas in a region specific study like the present one, there are latitudinal variability in primary production and surface temperature in this region. In this study, the discrepancy between estimated and modeled export flux estimates for the Laws and Dunne models could be due to time lag between primary production and subsequent carbon export due to seasonal changes in dominating phytoplankton groups in the Arabian Sea and the Indian Ocean (Buesseler et al., 2007; Maiti et al., 2016). Henson et al. (2015) described that the current empirical algorithms that consider only temperature were simple and resulted in large variability in export efficiency with increased primary production and needed to consider the carbon fraction carried by slow-sinking particles. The Arabian Sea experiences strong seasonal variability in primary production and changes in phytoplankton community and subsequent export. Ramaiah et al. (1996) showed that the Arabian

Sea was dominated by picoplankton community in February and consequently followed by high bacterial abundances in April-May. Change in phytoplankton community from diatoms during winter monsoon to picoplankton in February followed by bacterial abundance in April-May indicated the strong seasonal food web structure with a possible decrease in primary production, particle size and carbon export in the Arabian Sea (Sawant and Madhupratap, 1996; Bhattathiri et al., 1996). Although a lot of comparisons were made in different major world oceans, between ^{234}Th based and modeled estimates, these results are the first comparison made in the Indian Ocean.

The differences between modeled and in situ estimates found in the present study were similar to those reported for the Southern Ocean (Maiti et al., 2013), North Pacific Ocean (Stukel et al., 2015), and for global ocean models (Henson et al., 2011, 2015). Reasons for such disagreement between modeled and ^{234}Th based export efficiencies could include the time lag between production and export usually due to small phytoplankton communities, vertical migration of zooplankton that transfers carbon from surface and the export of DOC (Buesseler et al., 2007; Moran et al., 2012; Baumann et al., 2013; Henson et al., 2015; Laws et al., 2000; Maiti et al., 2016). A recent study quantified the temporal lag between primary production and export and revealed that the export efficiency highly varied at regions with strong seasonal variability in primary production (Henson et al., 2015). The current empirical algorithms for export efficiency that only consider temperature are overly simple and extrapolating carbon export from these models can result in error of up to $\pm 60\%$ (Henson et al., 2015).

5. Conclusion

The amount of organic carbon exported out of the ocean's euphotic zone, and its rate of remineralization in the mesopelagic zone, determines the amount of carbon sequestered in the deep ocean by the ocean's biological carbon pump. We have used the $^{234}\text{Th}/^{238}\text{U}$ proxy to estimate POC fluxes in the Arabian Sea and Indian Ocean along 65°E transect. The primary production varied from $58 \pm 3 \text{ mmol C m}^{-2} \text{ d}^{-1}$ to $179 \pm 9 \text{ mmol C m}^{-2} \text{ d}^{-1}$ and the ^{234}Th based POC export fluxes in the study region varied from negligible to $9.0 \pm 0.8 \text{ mmol C m}^{-2} \text{ d}^{-1}$. In contrast to the episodic decrease of primary production from 17°N to 16°S , ^{234}Th derived POC export fluxes show high values in the Indian Ocean. The ^{234}Th deficit in subsurface depths in this region is due to the diel vertical migration, grazing and fecal pellet production by mesozooplankton.

In addition, very few ^{234}Th studies are able to get in situ NPP measurements at the same time and so this study is uniquely able to assess production and export with both in-situ and satellite based estimates in one of the most dynamic regions of the upper ocean. Estimates of POC export fluxes

with empirical models and satellite observations of net primary production in the euphotic zone cannot determine the attenuation of the organic carbon flux with depth due to microbial loop and their predictions vary widely when compared among different models and with ^{234}Th tracer based estimates. The ^{234}Th based POC export flux is similar to the estimates from Henson model while Laws and Dunne models show comparatively higher export flux in the Arabian Sea and the Indian Ocean. Significant uncertainties remain especially on seasonal cycle in biological productivity that will need to be constrained by both improved models and increased observations.

Acknowledgements

This study was conducted as a part of the GEOTRACES programme, funded by Ministry of Earth Science, Government of India, New Delhi. We thank both the captain and the crew of the ORV SagarKanya (SK312) for their support during sample collection. We express thanks to Mr. Muruganandam, Pondicherry University, Port Blair for the enthusiastic help during the cruise. We are thankful to the two anonymous reviewers for their critical comments and valuable suggestions that considerably improved the manuscript. The data used are listed in the tables.

References

- Anand, S. S., R. Rengarajan, V. V. S. S. Sarma, A. K. Sudheer, R. Bhushan, and S. K. Singh (2017), Spatial variability of upper ocean POC export in the Bay of Bengal and the Indian ocean determined using particle-reactive ^{234}Th , *J. Geophys. Res. Oceans*, 122(5), 3753-3770, doi:10.1002/2016JC012639.
- Anand, S. S., R. Rengarajan, D. Shenoy, M. Gauns, S.W.A. Naqvi (2018), POC export fluxes in the Arabian Sea and the Bay of Bengal: A simultaneous $^{234}\text{Th}/^{238}\text{U}$ and $^{210}\text{Po}/^{210}\text{Pb}$ study, *Mar. Chem.*, 198, 70-87, doi.org/10.1016/j.marchem.2017.11.005.
- Barber, R. T., J. Marra, R. C. Bidigare, L. A. Codispoti, D. Halpern, Z. Johnson, M. Latasa, R. Goericke, and S. L. Smith (2001), Primary productivity and its regulation in the Arabian Sea during 1995, *Deep Sea Res., Part II*, 48, 1127–1172.
- Baumann, M.S., S.B. Moran, M.W. Lomas, R.P. Kelly, and D.W. Bell, (2013), Seasonal decoupling of particulate organic carbon export and net primary production in relation to sea-ice at the shelf break of the eastern Bering Sea: Implications for off-shelf carbon export, *J. Geophys. Res. Oceans*, 118(10), 5504-5522.
- Beal, L. M., V. Hormann, R. Lumpkin, and G. R. Foltz (2013), The response of the surface circulation of the Arabian Sea to monsoonal forcing, *J. Phys. Oceanogr.*, 43(9), 2008–2022, doi:10.1175/Jpo-D-13-033.1.
- Bhattathiri, P.M.A., A. Pant, S.S. Sawant, M. Gauns, S.G.P. Matondkar, and R. Mahanraju, (1996), Phytoplankton production and chlorophyll distribution in the eastern and central Arabian Sea in 1994-1995, *Curr. Sci.*, 71(11), 857-862.

- Black, E.E., K. O. Buesseler, S. M. Pike, and P. J. Lam(2017), ^{234}Th as a tracer of particulate export and remineralization in the Southeastern Tropical Pacific. *Mar. Chem.*, doi: 10.1016/j.marchem.2017.06.009.
- Buesseler, K., L. Ball, J. Andrews, C. Benitez-Nelson, R. Belostock, F. Chai, and Y. Chao (1998), Upper ocean export of particulate organic carbon in the Arabian Sea derived from thorium-234, *Deep Sea Res., Part II*, 45(10), 2461 - 2487, doi:10.1016/S0967-0645(98)80022-2.
- Buesseler, K.O., C. R. Benitez-Nelson, S. B. Moran, A. Burd, M. Charette, J. K. Cochran, L. Coppola, N. S. Fisher, S. W. Fowler, W. D. Gardner, L. D. Guo, O. Gustafsson, C. Lamborg, P. Masque, J. C. Miquel, U. Passow, P. H. Santschi, N. Savoye, G. Stewart, and T. Trull(2006), An assessment of particulate organic carbon to thorium-234 ratios in the ocean and their impact on the application of ^{234}Th as a POC flux proxy. *Mar. Chem.*, 100, 213–233.
- Buesseler, K. O. (1998), The decoupling of production and particulate export in the surface ocean, *Global Biogeochem. Cycles*, 12(2), 297 - 310, doi:10.1029/97GB03366.
- Buesseler, K.O., A.N. Antia, M. Chen, S.W. Fowler, W.D. Gardner, O. Gustafsson, K. Harada, A.F. Michaels, M. Rutgers van der Loeff, M. Sarin, and D.K. Steinberg (2007), An assessment of the use of sediment traps for estimating upper ocean particle fluxes, *J. Mar. Res.*, 65(3), 345-416.
- Buesseler, K. O., M. P. Bacon, J. K. Cochran, and H. D. Livingston (1992), Carbon and nitrogen export during the JGOFS north Atlantic bloom experiment estimated from ^{234}Th : ^{238}U disequilibria, *Deep Sea Res., Part A*, 39(7), 1115 - 1137, doi:10.1016/0198-0149(92)90060-7.
- Buesseler, K. O., C. Benitez-Nelson, M. R. van der Loeff, J. Andrews, L. Ball, G. Crossin, and M. A. Charette (2001), An inter-comparison of small- and large-volume techniques for thorium-234 in seawater, *Mar. Chem.*, 74(1), 15 - 28, doi:10.1016/S0304-4203(00)00092-X.
- Buesseler, K.O., S. Pike, K. Maiti, C. H. Lamborg, D. A. Siegel, and T. W. Trull (2009), Thorium-234 as a tracer of spatial, temporal and vertical variability in particle flux in the North Pacific. *Deep Sea Res. Part I*, 56(7), 1143-1167.
- Cai, P.H., M. H. Dai, W. H. Chen, T. T. Tang, and K. B. Zhou (2006a), On the importance of the decay of ^{234}Th in determining size fractionated C/Th-234 ratio on marine particles. *Geophys. Res. Lett.* 33, L23602. doi: 10.1029/2006g1027792.
- Cai, P., M. Dai, D. Lv, and W. Chen (2006b), An improvement in the small-volume technique for determining thorium-234 in seawater, *Mar. Chem.*, 100(3-4), 282 - 288, doi: 10.1016/j.marchem.2005.10.016.
- Cai, P., D. Zhao, L. Wang, B. Huang, and M. Dai(2015), Role of particle stock and phytoplankton community structure in regulating particulate organic carbon export in a large marginal sea. *J. Geophys. Res. Oceans*, 120, 2063–2095. doi: 10.1002/2014JC010432.
- Cochran J.K. (1992), The oceanic chemistry of the uranium and thorium-series nuclides *In: Uranium-series disequilibrium: applications to earth, marine, and environmental sciences*. Ivanovich M, Harmon R.S. (eds) Oxford University Press, New York, 334-395.

- DeVries, T., and T. Weber (2017), The export and fate of organic matter in the ocean: New constraints from combining satellite and oceanographic tracer observations, *Global Biogeochem. Cycles*, *31*, 535–555, doi:10.1002/2016GB005551.
- Dickey, T., J. Marra, D. E. Sigurdson, R. A. Weller, C. S. Kinkade, S. E. Zedler, J. D. Wiggert, and C. Langdon (1998), Seasonal variability of bio-optical and physical properties in the Arabian Sea: October 1994–October 1995. *Deep Sea Res., Part II*, *45*(10-11), 2001-2025.
- Dunne, J. P., R. A. Armstrong, A. Gnanadesikan, and J. L. Sarmiento (2005), Empirical and mechanistic models for the particle export ratio, *Global Biogeochem. Cycles*, *19*(4), doi:10.1029/2004GB002390, gB4026.
- Flagg, C. N., and H. S. Kim (1998), Upper ocean currents in the northern Arabian Sea from shipboard ADCP measurements collected during the 1994–1996 US JGOFS and ONR programs. *Deep Sea Res., Part II*, *45*(10-11), 1917-1959.
- Gauns, M., M. Madhupratap, N. Ramaiah, R. Jyothibabu, V. Fernands, J. T. Paul, and S. P. Kumar (2005), Comparative accounts of biological productivity characteristics and estimates of carbon fluxes in the Arabian Sea and the Bay of Bengal, *DeepSea Res., Part II*, *52*, 2003-2017.
- Gauns, M., R. Mohanraju, and M. Madhupratap (1996), Studies on the microzooplankton from the central and eastern Arabian Sea, *Curr. Sci.*, *71*, 874-877.
- Geider, R. J., C. M. Moore, and D. J. Suggett (2014). “Ecology of Marine Phytoplankton,” in *Ecology and the Environment*, ed. R. K. Monson (New York, NY: Springer Science+Business Media), 483–531.
- Hama, T., T. Miyazaki, Y. Ogawa, T. Iwakuma, M. Takahashi, A. Otsuki, and S. Ichimura (1983), Measurement of photosynthetic production of a marine phytoplankton population using a stable ^{13}C isotope, *Mar. Biol.*, *73*(1), 31-36, doi:10.1007/BF00396282.
- Haskell II, W. Z., D. Kadko, D. E. Hammond, A. N. Knapp, M. G. Prokopenko, W. M. Berelson, and D. G. Capone (2015), Upwelling velocity and eddy diffusivity from ^7Be measurements used to compare vertical nutrient flux to export POC flux in the eastern tropical south pacific, *Mar. Chem.*, *168*, 140 - 150, doi:10.1016/j.marchem.2014.10.004.
- Henson, S. A., R. Sanders, E. Madsen, P. J. Morris, F. Le Moigne, and G. D. Quartly (2011), A reduced estimate of the strength of the ocean's biological carbon pump, *Geophys. Res. Lett.*, *38* (4), doi:10.1029/2011GL046735, 104606.
- Henson, S. A., R. Sanders, and E. Madsen (2012), Global patterns in efficiency of particulate organic carbon export and transfer to the deep ocean, *Global Biogeochem. Cycles*, *26*(1), doi:10.1029/2011GB004099, gB1028.
- Henson, S.A., A. Yool, and R. Sanders (2015), Variability in efficiency of particulate organic carbon export: A model study, *Global Biogeochem. Cycles*, *29*(1), 33-45.
- Honjo, S. (1996). Fluxes of particles to the interior of the open oceans. In: Ittekkot, V., P. Schafer, S. Honjo, P. J. Depetris (Eds.), *Particle Flux in the Ocean*, Scope vol. 57. Wiley, New York, pp. 91-154.

- Honjo, S., J. Dymond, W. Prell, and V. Ittekkot (1999), Monsoon-controlled export fluxes to the interior of the Arabian Sea, *Deep Sea Res., Part II*, 46(8), 1859-1902.
- Hung, C. C., L. D. Guo, K. A. Roberts, and P. H. Santschi (2004), Upper ocean carbon flux determined by size-fractionated ^{234}Th data and sediment traps in the Gulf of Mexico. *Geochem. J.*, 38, 601–611.
- Hung, C. C., G. C. Gong, and P. H. Santschi (2012) ^{234}Th in different size classes of sediment trap collected particles from the Northwestern Pacific Ocean. *Geochim. Cosmochim. Acta*, 91, 60–74.
- Kothawale, D. R., A. A. Munot, and H. P. Borgaonkar (2007), Temperature variability over the Indian Ocean and its relationship with Indian summer monsoon rainfall. *Theor. Appl. Climatol.*, 92, 31-45.
- Kumar, S. P., and T. G. Prasad (1999), Formation and spreading of Arabian Sea high salinity water mass, *J. Geophys. Res. Oceans*, 104(C1), 1455 - 1464, doi: 10.1029/1998JC900022.
- Kumar, S. P., and J. Narvekar (2005), Seasonal variability of the mixed layer in the central Arabian Sea and its implication on nutrients and primary productivity, *Deep Sea Res., Part II*, 52, 1848-1861.
- Latasa, M., and R. R. Bidigare (1998), A comparison of phytoplankton populations of the Arabian Sea during the Spring Intermonsoon and Southwest Monsoon of 1995 as described by HPLC-analyzed pigments, *Deep Sea Res., Part II*, 45, 2133–2170.
- Laws, E. A., P. G. Falkowski, W. O. Smith, H. Ducklow, and J. J. McCarthy (2000), Temperature effects on export production in the open ocean, *Global Biogeochem. Cycles*, 14(4), 1231 - 1246, doi:10.1029/1999GB001229.
- Laws, E. A., E. D'Sa, and P. Naik (2011), Simple equations to estimate ratios of new or export production to total production from satellite-derived estimates of sea surface temperature and primary production, *Limnol. Oceanogr. Methods*, 9(12), 593 - 601, doi: 10.4319/lom.2011.9.593.
- Le Moigne, F. A. C., S. A. Henson, R. J. Sanders, and E. Madsen (2013), Global database of surface ocean particulate organic carbon export fluxes diagnosed from the ^{234}Th technique, *Earth Syst. Sci. Data*, 5(2), 295 - 304, doi:10.5194/essd-5-295-2013.
- Liu, Z., G. Stewart, J. K. Cochran, C. Lee, R. A. Armstrong, D. J. Hirschberg, B. Gasser, and J. C. Miquel, (2005), Why do POC concentrations measured using Niskin bottle collections sometimes differ from those using in-situ pumps?, *Deep Sea Res., Part I*, 52(7), 1324-1344.
- Liu, Z., J. K. Cochran, C. Lee, B. Gasser, J. C. Miquel, and S. G. Wakeham (2009), Further investigations on why POC concentrations differ in samples collected by Niskin bottle and in situ pump, *Deep Sea Res., Part II*, 56(18), 558-1567.
- Madhupratap, M., S.P. Kumar, P.M.A. Bhattathiri, M.D. Kumar, S. Raghukumar, K.K.C. Nair, and N. Ramaiah (1996), Mechanisms of the biological response to winter cooling in the northeastern Arabian Sea. *Nature*, 384(6609), 349-352.

- Maiti, K., S. Bosu, E. D'Sa, P. Adhikari, M. Sutor, and K. Longnecker (2016), Export fluxes in northern Gulf of Mexico - comparative evaluation of direct, indirect and satellite-based estimates, *Mar. Chem.*, 184, 60 - 77, doi:10.1016/j.marchem.2016.06.001.
- Maiti, K., M.A. Charette, K.O. Buesseler, and M. Kahru (2013), An inverse relationship between production and export efficiency in the Southern Ocean, *Geophys. Res. Lett.*, 40(8), 1557-1561.
- McCreary, J.P., Z. Yu, R. R. Hood, and P. Vinayachandran, R. Furue, A. Ishida, and K. J. Richards (2013), Dynamics of the Indian-Ocean oxygen minimum zones, *Prog. Oceanogr.*, 112-113, 15-37.
- Mohan, R., K. Verma, L. P. Mergulhao, D. K. Sinha, S. Shanvas, and M. V. S. Gupta (2006), Seasonal variation of pteropods from the western Arabian Sea sediment trap, *Geo-Marine Lett.*, 26(5), 265 - 273, doi:10.1007/s00367-006-0035-1.
- Moran, S.B., M. A. Charette, S. M. Pike, and C. A. Wicklund, (1999), Differences in seawater particulate organic carbon concentration in samples collected using small-and large-volume methods: the importance of DOC adsorption to the filter blank, *Mar. Chem.*, 67(1-2), 33-42.
- Moran, S.B., M.W. Lomas, R.P. Kelly, R. Gradinger, K. Iken, and J.T. Mathis (2012), Seasonal succession of net primary productivity, particulate organic carbon export, and autotrophic community composition in the eastern Bering Sea, *Deep Sea Res. Part II*, 65, 84-97.
- Naqvi, S.W.A. (1994), Denitrification processes in the Arabian Sea, *Proc. Indian Acad. Sci. (Earth Planet. Sci.)*, 103(2), 279-300.
- Naqvi, S.W.A. and R.J. Noronha (1991), Nitrous oxide in the Arabian Sea. *Deep Sea Res.*, 38(7), 871-890.
- Olli, K., P. Wassmann, M. Reigstad, T.N. Ratkova, E. Arashkevich, A. Pasternak, P.A. Matrai, J. Knulst, L. Tranvik, R. Klais, and A. Jacobsen (2007), The fate of production in the central Arctic Ocean—top–down regulation by zooplankton expatriates?. *Progr. Oceanogr.*, 72(1), 84-113.
- Owens, S., K. Buesseler, and K. Sims (2011), Re-evaluating the ^{238}U -salinity relationship in seawater: Implications for the ^{238}U - ^{234}Th disequilibrium method, *Mar. Chem.*, 127, 31 - 39, doi:http://dx.doi.org/10.1016/j.marchem.2011.07.005.
- Pates, J.M., and G.K.P. Muir (2007), U–salinity relationships in the Mediterranean: Implications for ^{234}Th : ^{238}U particle flux studies, *Mar. Chem.*, 106(3), 530-545.
- Prasad, T. G., M. Ikeda, and S. P. Kumar (2001), Seasonal spreading of the Persian Gulf Water mass in the Arabian Sea, *J. Geophys. Res.*, 106(C8), 17059–17071, doi:10.1029/2000JC000480.
- Puigcorb , V., C. R. Benitez-Nelson, P. Masqu , E. Verdeny, A. E. White, B. N. Popp, F. G. Prahl, and P. J. Lam (2015), Small phytoplankton drive high summertime carbon and nutrient export in the Gulf of California and Eastern Tropical North Pacific, *Global Biogeochem. Cycles*, 29, 1309–1332, doi:10.1002/2015GB005134.
- Qasim, S.Z. (1982), Oceanography of the northern Arabian Sea, *Deep Sea Res.*, 29(9), 1041-1068.
- Ramaiah, N., S. Raghukumar, and M. Gauns (1996), Bacterial abundance and production in the central and eastern Arabian Sea, *Curr. Sci.*, 71(11), 878 – 882.

- Rengarajan, R., M.M. Sarin, and S. Krishnaswami (2003), Uranium in the Arabian Sea: role of denitrification in controlling its distribution, *Oceanol. acta*, 26(5), 687-693.
- Richardson, T.L. and G.A. Jackson (2007), Small phytoplankton and carbon export from the surface ocean, *Science*, 315(5813), 838-840.
- Riebesell, U., K. G. Schulz, R. G. J. Bellerby, M. Botros, P. Fritsche, M. Meyerhöfer, et al. (2007). Enhanced biological carbon consumption in a high CO₂ ocean. *Nature*, 450, 545–549. doi: 10.1038/nature06267
- Rodriguez y Baena, A.M., S. W. Fowler, and J. C. Miquel (2007), Particulate organic carbon: natural radionuclide ratios in zooplankton and their freshly produced fecal pellets from the NW Mediterranean (MedFlux 2005). *Limnol. Oceanogr.*, 52(3), 966–974.
- Roman, M., S. Smith, K. Wishner, X. Zhang, and M. Gowing (2000), Mesozooplankton production and grazing in the Arabian Sea, *Deep Sea Res., Part II*, 47(7), 1423-1450.
- Roullier, F., L. Berline, L. Guidi, X. Durrieu De Madron, M. Picheral, A. Sciandra, S. Pesant, and L. Stemann (2014), Particle size distribution and estimated carbon flux across the Arabian Sea oxygen minimum zone, *Biogeosciences*, 11(16), 4541 - 4557, doi:10.5194/bg-11-4541-2014.
- Rutgers van der Loeff, M., M. M. Sarin, M. Baskaran, C. Benitez-Nelson, K. O. Buesseler, M. Charette, M. Dai, O. Gustafsson, P. Masque, P. J. Morris, K. Orlandini, A. Rodriguez y Baena, N. Savoye, S. Schmidt, R. Turnewitsch, I. Voge, and J. T. Waples (2006), A review of present techniques and methodological advances in analyzing ²³⁴Th in aquatic systems, *Mar. Chem.*, 100(3-4), 190-212.
- Sarin, M., S. Krishnaswami, R. Ramesh, and B. Somayajulu (1994), ²³⁸U decay series nuclides in the northeastern Arabian sea: Scavenging rates and cycling processes, *Continental Shelf Res.*, 14 (2), 251 - 265, doi:10.1016/0278 - 4343(94)90015-9.
- Sarin, M. M., R. Rengarajan, and V. Ramaswamy (1996), ²³⁴Th scavenging and particle export fluxes from the upper 100 m of the Arabian Sea, *Curr. Sci.*, 71(11), 888 - 893.
- Sarma, V. V. S. S., M. D. Kumar, M. D. George, and A. Rajendran (1996), Seasonal variations in inorganic carbon components in the central and eastern Arabian sea, *Curr. Sci.*, 71(11), 852 - 856.
- Sarma, V.V.S.S., G. D. Rao, R. Viswanadham, C. K. Sherin, J. Salisbury, M. M. Omand, A. Mahadevan, V. S. N. Murty, E. L. Shroyer, M. Baumgartner, and K. M. Stafford (2016), Effects of freshwater stratification on nutrients, dissolved oxygen, and phytoplankton in the Bay of Bengal. *Oceanography*, 29(2), 222-231.
- Sarma, V.V.S.S., P. S. Swathi, M. D. Kumar, S. Prasanna Kumar, P. M. A. Bhattathiri, M. Madhupratap, V. Ramaswamy, M. M. Sarin, M. Gauns, N. Ramaiah, S. Sardesai, and S. N. deSousa (2003), Carbon budget in the eastern and central Arabian Sea: an Indian JGOFS synthesis. *Global Biogeochem. Cycle* 17, 1102, doi:10.1029/1002GB001978.
- Sawant, S., and M. Madhupratap (1996), Seasonality and composition of phytoplankton in the Arabian Sea, *Curr. Sci.*, 71(11), 869 - 873.

Schott, F. A., S. P. Xie, and J. P. McCreary (2009), Indian Ocean circulation and climate variability, *Rev. Geophys.*, 47(1), doi:10.1029/2007RG000245, rG1002.

Shetye, S.R., A.D. Gouveia, and S.S.C. Shenoi (1994), Circulation and water masses of the Arabian Sea. *Proc. Indian Acad. Sci.(Earth Planet. Sci.)*, 103(2), 107-123.

Stukel, M.R., M. Kahru, C.R. Benitez-Nelson, M. Décima, R. Goericke, M.R. Landry, and M.D. Ohman, (2015), Using Lagrangian-based process studies to test satellite algorithms of vertical carbon flux in the eastern North Pacific Ocean, *J. Geophys. Res. Oceans*, 120(11), 7208-7222.

Thomalla, S. J., A. J. Poulton, R. Sanders, R. Turnewitsch, P. M. Holligan, and M. I. Lucas (2008), Variable export fluxes and efficiencies for calcite, opal, and organic carbon in the Atlantic Ocean: A ballast effect in action?, *Global Biogeochem. Cycles*, 22(1), doi: 10.1029/2007GB002982, gB1010.

Vinayachandran, P.N., and S. R. Shetye(1991),The warm pool in the Indian Ocean. *Proc. Indian Acad. Sci. (Earth Planet Sci.)*, 100, 165-175, <https://doi.org/10.1007/BF02839431>.

Webster, P.J., A.M. Moore, J.P. Loschnigg, and R.R. Leben (1999), Coupled ocean–atmosphere dynamics in the Indian Ocean during 1997–98, *Nature*, 401(6751), 356-360.

Wei, C.L., Lin, S.Y., Sheu, D.D.D., Chou, W.C., Yi, M.C., Santschi, P.H., Wen, L.S., 2011. Particle-reactive radionuclides (^{234}Th , ^{210}Pb , ^{210}Po) as tracers for the estimation of export production in the south China Sea. *Biogeosciences*, 8, 3793–3808. doi:10.5194/bg-8-3793-2011.

Wishner, K.F., M.M. Gowing, and C. Gelfman (1998), Mesozooplankton biomass in the upper 1000m in the Arabian Sea: overall seasonal and geographic patterns, and relationship to oxygen gradients, *Deep Sea Res., Part II*, 45(10-11), 2405-2432.

Wyrtki K. (1973), An equatorial jet in the Indian Ocean,*Science*, 181, 262-264.

Xu, C., P. H. Santschi, C. C. Hung, S. Zhang, K. A. Schwehr, K. A. Roberts, L. D. Guo, G. C. Gong, A. Quigg, R. Long, J. Pinckney, S. W. Duan, R. Amon, C. L. Wei (2011), Controls of Th-234 removal from the oligotrophic ocean by polyuronic acids and modification by microbial activity, *Mar. Chem.*, 123, 111–126.

Zhou, K., K. Maiti, M. Dai, S. J. Kao, and K. Buesseler, (2016), Does adsorption of dissolved organic carbon and thorium onto membrane filters affect the carbon to thorium ratios, a primary parameter in estimating export carbon flux?, *Mar. Chem.*, 184, 1-10.

Table 1

Station details (location, total water column depth and date of collection), depth, temperature, salinity, ^{238}U , total ^{234}Th and the total $^{234}\text{Th}/^{238}\text{U}$ ratio for the SK312 cruise along the GEOTRACES GI02 section in the Arabian Sea and Indian Ocean. Standard deviations of radionuclide data are based on counting error (1σ).

Depth (m)	Pot. Temp. (°C)	Salinity (psu)	^{238}U (dpm L ⁻¹)	^{234}Th (dpm L ⁻¹)	$^{234}\text{Th}/^{238}\text{U}$ (A.R.)
Sta. 8, 16° 01.08'S, 65° 00.04'E; 3182 m, 09.5.2014					
2	27.253	34.893	2.49 ± 0.07	2.98 ± 0.08	1.20 ± 0.05
10	27.259	34.830	2.48 ± 0.07	2.63 ± 0.07	1.06 ± 0.04
25	27.253	34.876	2.49 ± 0.07	2.29 ± 0.06	0.92 ± 0.04
50	27.066	34.886	2.49 ± 0.07	3.09 ± 0.08	1.24 ± 0.05
75	23.745	35.021	2.50 ± 0.07	2.95 ± 0.07	1.18 ± 0.05
100	22.965	35.021	2.50 ± 0.07	2.70 ± 0.07	1.08 ± 0.04
150	22.442	35.054	2.50 ± 0.07	2.63 ± 0.07	1.05 ± 0.04
200	20.117	35.472	2.53 ± 0.08	2.66 ± 0.07	1.05 ± 0.04
300	14.925	35.388	2.52 ± 0.08	2.84 ± 0.07	1.13 ± 0.04
2000	2.253	34.710	2.47 ± 0.07	2.71 ± 0.09	1.10 ± 0.05
Sta. 9, 12° 00.06'S, 64° 59.98'E; 3449 m, 11.5.2014					
2	27.840	34.577	2.47 ± 0.07	2.27 ± 0.07	0.92 ± 0.04
10	27.858	34.679	2.47 ± 0.07	2.38 ± 0.07	0.96 ± 0.04
25	27.827	34.702	2.47 ± 0.07	1.33 ± 0.05	0.54 ± 0.03
50	24.150	35.049	2.50 ± 0.08	1.11 ± 0.04	0.43 ± 0.02
75	20.894	35.223	2.51 ± 0.08	1.69 ± 0.05	0.67 ± 0.03
100	20.694	35.527	2.53 ± 0.08	2.38 ± 0.06	0.94 ± 0.04
150	17.215	35.366	2.52 ± 0.08	1.73 ± 0.05	0.69 ± 0.03
200	14.123	35.172	2.51 ± 0.08	2.25 ± 0.06	0.90 ± 0.04
300	11.311	34.937	2.49 ± 0.07	2.36 ± 0.06	0.95 ± 0.04
Sta. 10, 08° 1.09'S, 66° 41.43'E; 4161 m, 13.5.2014					
2	28.737	33.619	2.40 ± 0.07	2.00 ± 0.06	0.84 ± 0.04
10	28.740	33.781	2.41 ± 0.07	1.84 ± 0.05	0.76 ± 0.03
25	28.745	34.030	2.43 ± 0.07	1.55 ± 0.05	0.64 ± 0.03
50	24.247	35.211	2.51 ± 0.08	1.74 ± 0.05	0.69 ± 0.03
75	19.913	35.121	2.50 ± 0.08	2.05 ± 0.06	0.82 ± 0.03
100	18.190	35.111	2.50 ± 0.08	2.70 ± 0.06	1.08 ± 0.04
150	14.835	34.948	2.49 ± 0.07	2.30 ± 0.06	0.92 ± 0.04
200	13.103	34.947	2.49 ± 0.07	2.00 ± 0.05	0.80 ± 0.03
300	11.118	34.920	2.49 ± 0.07	2.10 ± 0.06	0.85 ± 0.03
Sta. 11, 05° 16.05'S, 67° 54.01'E; 3000 m, 14.5.2014					
2	29.295	34.467	2.46 ± 0.07	2.03 ± 0.06	0.83 ± 0.03
10	29.295	34.471	2.46 ± 0.07	1.64 ± 0.06	0.67 ± 0.03
25	28.355	35.136	2.51 ± 0.08	1.62 ± 0.05	0.65 ± 0.03
50	23.466	35.245	2.51 ± 0.08	1.30 ± 0.05	0.52 ± 0.02
75	19.264	35.276	2.52 ± 0.08	2.19 ± 0.06	0.87 ± 0.04
100	17.513	35.269	2.51 ± 0.08	2.88 ± 0.06	1.15 ± 0.04
150	14.417	35.168	2.51 ± 0.08	2.41 ± 0.06	0.96 ± 0.04
200	13.296	35.089	2.50 ± 0.08	2.32 ± 0.06	0.93 ± 0.04
300	11.024	34.941	2.49 ± 0.07	2.58 ± 0.06	1.03 ± 0.04

Sta. 12, 0° 0.408'S, 65° 0.29'E; 3900 m, 16.5.2014

2	30.534	35.045	2.50 ± 0.07	2.07 ± 0.06	0.83 ± 0.03
10	30.480	35.262	2.51 ± 0.08	1.88 ± 0.07	0.75 ± 0.04
25	30.411	35.258	2.51 ± 0.08	1.84 ± 0.05	0.73 ± 0.03
50	29.810	35.298	2.52 ± 0.08	1.85 ± 0.05	0.74 ± 0.03
75	27.370	35.585	2.54 ± 0.08	2.17 ± 0.06	0.86 ± 0.04
100	22.179	35.473	2.53 ± 0.08	2.50 ± 0.06	0.99 ± 0.04
150	16.568	35.264	2.51 ± 0.08	1.99 ± 0.05	0.79 ± 0.03
200	13.331	35.148	2.51 ± 0.08	1.71 ± 0.05	0.68 ± 0.03
300	12.047	35.080	2.50 ± 0.08	1.86 ± 0.05	0.74 ± 0.03

Sta. 13, 3° 59.85'N, 64° 59.99'E; 3800 m, 18.5.2014

2	30.510	34.766	2.48 ± 0.07	2.13 ± 0.06	0.86 ± 0.04
10	30.466	34.802	2.48 ± 0.07	1.69 ± 0.05	0.68 ± 0.03
25	30.390	34.800	2.48 ± 0.07	1.34 ± 0.06	0.54 ± 0.03
50	28.467	35.149	2.51 ± 0.08	1.08 ± 0.05	0.43 ± 0.02
75	25.884	35.519	2.53 ± 0.08	1.55 ± 0.05	0.61 ± 0.03
100	22.521	35.438	2.53 ± 0.08	2.71 ± 0.06	1.07 ± 0.04
150	17.422	35.218	2.51 ± 0.08	2.15 ± 0.05	0.86 ± 0.03
200	13.895	35.216	2.51 ± 0.08	1.96 ± 0.05	0.78 ± 0.03
300	11.765	35.129	2.50 ± 0.08	2.15 ± 0.06	0.86 ± 0.03

Sta. 14, 6° 59.87'N, 64° 59.91'E; 4858 m, 20.5.2014

2	31.060	34.548	2.46 ± 0.07	2.39 ± 0.06	0.97 ± 0.04
10	31.022	34.638	2.47 ± 0.07	2.23 ± 0.06	0.90 ± 0.04
25	29.471	35.168	2.51 ± 0.08	1.69 ± 0.05	0.67 ± 0.03
50	28.578	35.678	2.54 ± 0.08	1.28 ± 0.04	0.51 ± 0.02
75	26.977	36.452	2.60 ± 0.08	1.72 ± 0.05	0.66 ± 0.03
100	23.836	35.802	2.55 ± 0.08	1.50 ± 0.05	0.59 ± 0.03
150	17.992	35.371	2.52 ± 0.08	1.93 ± 0.05	0.77 ± 0.03
200	14.950	35.217	2.51 ± 0.08	1.69 ± 0.05	0.67 ± 0.03
300	12.644	35.199	2.51 ± 0.08	1.62 ± 0.05	0.65 ± 0.03

Sta. 15^a, 9° 59.92'N, 65° 00.02'E; 4543 m, 21.5.2014

2	30.864	34.271	2.44 ± 0.07	2.28 ± 0.06	0.93 ± 0.04
10	30.854	34.312	2.45 ± 0.07	1.82 ± 0.06	0.75 ± 0.03
25	30.762	34.308	2.45 ± 0.07	1.41 ± 0.05	0.58 ± 0.03
50	29.074	34.874	2.49 ± 0.07	1.34 ± 0.05	0.54 ± 0.03
75	28.535	35.890	2.56 ± 0.08	1.49 ± 0.05	0.58 ± 0.03
100	27.692	36.119	2.58 ± 0.08	2.23 ± 0.06	0.87 ± 0.04
150	21.201	35.625	2.54 ± 0.08	2.27 ± 0.06	0.90 ± 0.04
200	15.938	35.174	2.51 ± 0.08	1.84 ± 0.05	0.73 ± 0.03
300	13.344	35.350	2.52 ± 0.08	1.81 ± 0.05	0.72 ± 0.03

Sta. 16, 12° 59.94'N, 65° 00.04'E; 4203 m, 23.5.2014

2	30.993	36.054	2.57 ± 0.08	2.34 ± 0.06	0.91 ± 0.04
10	30.998	36.201	2.58 ± 0.08	1.89 ± 0.06	0.73 ± 0.03
25	29.259	36.488	2.60 ± 0.08	1.73 ± 0.06	0.67 ± 0.03
50	25.175	36.161	2.58 ± 0.08	1.44 ± 0.05	0.56 ± 0.03
75	24.972	36.343	2.59 ± 0.08	1.89 ± 0.05	0.73 ± 0.03
100	24.314	36.411	2.60 ± 0.08	2.50 ± 0.07	0.96 ± 0.04
150	18.611	35.771	2.55 ± 0.08	2.46 ± 0.06	0.96 ± 0.04
200	16.168	35.729	2.55 ± 0.08	2.20 ± 0.05	0.87 ± 0.03

300	13.400	35.522	2.53 ± 0.08	2.57 ± 0.07	1.01 ± 0.04
2000	2.765	34.813	2.48 ± 0.07	2.46 ± 0.07	0.99 ± 0.04
Sta. 17, 16° 00.01'N, 65° 00.01'E; 3797 m, 25.5.2014					
2	30.502	36.559	2.61 ± 0.08	2.20 ± 0.06	0.84 ± 0.04
10	30.487	36.618	2.61 ± 0.08	1.69 ± 0.05	0.65 ± 0.03
25	30.407	36.629	2.61 ± 0.08	1.44 ± 0.05	0.55 ± 0.03
50	25.495	36.151	2.58 ± 0.08	0.98 ± 0.05	0.38 ± 0.02
75	24.211	36.151	2.58 ± 0.08	1.67 ± 0.05	0.65 ± 0.03
100	24.201	36.340	2.59 ± 0.08	2.39 ± 0.06	0.92 ± 0.04
150	21.088	35.963	2.56 ± 0.08	1.83 ± 0.05	0.71 ± 0.03
200	18.208	35.811	2.55 ± 0.08	1.69 ± 0.05	0.66 ± 0.03
300	15.158	35.867	2.56 ± 0.08	1.68 ± 0.05	0.66 ± 0.03
Sta. 18^a, 17° 18.01'N, 69° 03.59'E; 3600 m, 28.5.2014					
2	30.336	36.630	2.61 ± 0.08	2.11 ± 0.06	0.81 ± 0.03
10	30.338	36.632	2.61 ± 0.08	1.67 ± 0.05	0.64 ± 0.03
25	30.078	36.641	2.61 ± 0.08	1.42 ± 0.05	0.54 ± 0.02
50	26.822	36.549	2.61 ± 0.08	1.06 ± 0.04	0.41 ± 0.02
75	25.132	36.495	2.60 ± 0.08	1.70 ± 0.05	0.65 ± 0.03
100	23.958	36.415	2.60 ± 0.08	2.23 ± 0.06	0.86 ± 0.03
150	20.443	35.999	2.57 ± 0.08	1.49 ± 0.05	0.58 ± 0.03
200	17.593	35.789	2.55 ± 0.08	1.69 ± 0.05	0.66 ± 0.03
300	14.438	35.654	2.54 ± 0.08	1.52 ± 0.05	0.60 ± 0.03

^a Data from Anand et al., 2018

Table. 2.

In situ primary production, ^{234}Th flux, particulate organic carbon, ^{234}Th and POC/ ^{234}Th ratio from sinking particulate matter are given for all the stations sampled along the GEOTRACES GI02 section in the Arabian Sea and Indian Ocean of the SK312 cruise. Also shown are the integrated fluxes of ^{234}Th and POC export fluxes with POC export efficiencies calculated up to 100 m and euphotic depth.

Sta. code	Position	Euphotic depth ^a (m)	In situ primary production ($\text{mmol m}^{-2} \text{d}^{-1}$)	POC ($\mu\text{mol L}^{-1}$)	Particulate ^{234}Th (dpm L^{-1})	POC/ ^{234}Th ($\mu\text{mol dpm}^{-1}$)	^{234}Th Flux ($\text{dpm m}^{-2} \text{d}^{-1}$)		POC Flux ($\text{mmol m}^{-2} \text{d}^{-1}$)		POC export efficiency (%)	
							(1)	(2)	(1)	(2)	(1)	(2)
8	16.00°S 64.99°E	145	58.4 ± 2.9	0.93 ± 0.03	0.31 ± 0.016	3.03 ± 0.182	(852) ± (99)	(1016) ± (135)	-	-	-	-
9	12.00°S 65.00°E	59	129.4 ± 6.5	0.79 ± 0.02	0.21 ± 0.015	3.77 ± 0.292	2373 ± 86	1504 ± 58	9.0 ± 0.8	5.7 ± 0.5	6.96	4.40
10	8.02°S 66.69°E	56	86.9 ± 4.3	0.53 ± 0.02	0.41 ± 0.018	1.29 ± 0.068	1575 ± 87	1126 ± 56	2.0 ± 0.2	1.5 ± 0.1	2.30	1.73
11	5.27°S 67.90°E	65	130.1 ± 6.5	1.09 ± 0.03	0.38 ± 0.018	2.84 ± 0.158	1827 ± 88	1780 ± 72	5.2 ± 0.4	5.0 ± 0.4	4.00	3.84
12	0.01°S 65.00°E	95	107.4 ± 5.4	0.72 ± 0.02	0.33 ± 0.017	2.17 ± 0.130	1424 ± 90	1361 ± 83	3.1 ± 0.3	3.0 ± 0.3	2.89	2.79
13	4.00°N 65.00°E	69	139.2 ± 7.0	0.40 ± 0.01	0.39 ± 0.018	1.02 ± 0.056	2645 ± 87	2109 ± 66	2.7 ± 0.2	2.2 ± 0.1	1.94	1.58
14	7.00°N 65.00°E	72	176.3 ± 8.8	0.95 ± 0.03	0.34 ± 0.017	2.84 ± 0.167	2484 ± 86	1657 ± 69	7.0 ± 0.5	4.7 ± 0.3	3.97	2.67
15	10.00°N 65.00°E	92	109.3 ± 5.5	0.58 ± 0.02	0.43 ± 0.018	1.36 ± 0.07	2545 ± 87	2371 ± 79	3.5 ± 0.2	3.2 ± 0.2	3.20	2.93
16	13.00°N 64.99°E	65	135.7 ± 6.8	1.00 ± 0.03	1.09 ± 0.026	0.91 ± 0.035	2127 ± 91	1554 ± 65	1.9 ± 0.1	1.4 ± 0.1	1.40	1.03
17	16.00°N 65.00°E	67	174.8 ± 8.7	0.43 ± 0.01	0.41 ± 0.018	1.04 ± 0.055	2926 ± 89	2213 ± 65	3.0 ± 0.2	2.3 ± 0.1	1.72	1.32
18	17.30°N 69.06°E	85	179.7 ± 9.0	1.27 ± 0.04	0.84 ± 0.024	1.51 ± 0.062	2980 ± 87	2658 ± 73	4.5 ± 0.2	4.0 ± 0.2	2.50	2.23

^a (DCM+10 m) is considered as the depth of euphotic zone (Haskell et al., 2015)

(1) - Integrated to 100 m depth

(2) - Integrated to euphotic depth

Values in parentheses are excess ^{234}Th released from biological remineralization of sinking particulate material.

For the modeled POC export flux calculations; in situ primary production, surface temperature and euphotic depth are used.

Table. 3.

Comparison of ^{234}Th based POC export flux measured in the Arabian Sea during spring intermonsoon.

Station code	Position	POC flux (mmol m⁻² d⁻¹)	Reference
TN045-N9	17.2 °N 68 °E	2.4	Buesseler et al. (1998)
SK312-18	17.3 °N 69 °E	4.5	This study
SK91-15N	15 °N 64 °E	30.9	Sarin et al. (1996)
TN045-S11	14.5 °N 65 °E	2.9	Buesseler et al. (1998)
SK312-16	13.0 °N 65 °E	1.9	This study
TN045-S13	12.0 °N 65 °E	0.3	Buesseler et al. (1998)
SK91-11N	11.0 °N 64 °E	26.8	Sarin et al. (1996)
SK312-15	10.0 °N 65 °E	3.5	This study
TN045-S15	9.9 °N 65 °E	2.7	Buesseler et al. (1998)

Table 4.

In situ and modeled, primary production and export efficiencies, for the Arabian Sea and Indian Ocean along the GEOTRACES GI02 section.

Primary production	Avg. productivity (mmol m ⁻² d ⁻¹)	Avg. export efficiency (%)			
		²³⁴ Th based	Laws model	Dunne model	Henson model
Arabian Sea					
In situ	155 ± 31	2.6 ± 1.1	16.2 ± 1.2	14.9 ± 1.9	2.0 ± 0.1
VGPM	23 ± 2	18 ± 9.8	9.0 ± 0.4	3.8 ± 1.3	2.0 ± 0.1
CbPM	47 ± 5	8.6 ± 4.4	11.3 ± 0.4	8.1 ± 1.4	2.0 ± 0.1
Indian Ocean					
In situ	108 ± 31	3.6 ± 2.0	15.5 ± 1.3	14.2 ± 3.3	2.3 ± 0.2
VGPM	18 ± 3	23.8 ± 15.0	9.0 ± 0.5	3.9 ± 2.8	2.3 ± 0.2
CbPM	44 ± 6	9.6 ± 6.3	11.8 ± 0.6	9.1 ± 2.8	2.3 ± 0.2

Figure captions

Figure 1. Station location and bathymetry map of the study region along the GEOTRACES GI02 section in the Arabian Sea and the Indian Ocean during April-May 2014.

Figure 2. Depth-latitude vertical sections of oxygen saturation (%) and CTD sensor parameters (Salinity and Temperature) with dissolved inorganic nutrients. Salinity (white contours) is shown relative to dissolved inorganic nitrogen (DIN) (a), Temperature (white contours) is shown relative to phosphate (b), density (white contours) is shown relative to silicate (c) and Oxygen saturation (white contours) is shown relative to fluorescence (d). The black contour lines represent the maximum depth of limiting nutrient.

Figure 3. TS diagram for all the stations sampled in the cruise SK312 with Indian Ocean water masses superimposed (based on Wyrski, 1971; Prasad et al. 2001). Abbreviations are ASHSW, Arabian Sea High Salinity Water mass; PGW, Persian Gulf Water; RSW, Red Sea Water mass.

Figure 4. Vertical (0-300 m depth) profiles of ^{234}Th (black line), ^{238}U (black-dash line), fluorescence (black dotted line) and dissolved oxygen (grey dash-line) measured at all the stations in the cruise.

Figure 5. Depth-latitude vertical sections of oxygen saturation (%) (white contour lines) is shown relative to (a) ^{234}Th , (b) ^{238}U and (c) $^{234}\text{Th}/^{238}\text{U}$ activity ratio.

Figure 6. Latitudinal variability of (a) in situ primary production, (b) POC, (c) particulate ^{234}Th , (d) POC/ ^{234}Th ratio, (e) ^{234}Th flux, (f) POC export flux and (g) POC export efficiency. ^{234}Th flux, POC flux and POC export efficiency of the southernmost station (Sta. 8 at 16°S) is not shown as there is no ^{234}Th deficit.

Figure 7. Comparison of latitudinal variation of in situ primary production with satellite data based NPP using VGPM and CbPM algorithms. Note there is no latitudinal change in modeled NPP values.

Figure 8. Plot showing relation between primary production and POC export flux: in situ primary production (a) along with satellite data based NPP estimates using VGPM (b) and CbPM (c) algorithms. The POC export flux out of the euphotic zone were derived by Laws, Dunne and Henson's models. Dashed trend lines represent export efficiencies of 2, 5, 10 and 20%.

Figure 9. Plot showing relation between primary production and POC export efficiency. ^{234}Th based POC export efficiency (filled circles) is plotted along with those derived from (i) Laws' model (open circle), (ii) Dunne's model (open square) and (iii) Henson's model (open triangle). Primary production from in situ measurements (a) as well as satellite data based NPP estimates using VGPM (b) and CbPM (c) algorithms are used to derive export efficiencies. Note that Henson model based POC export efficiencies are comparable with those derived using ^{234}Th .

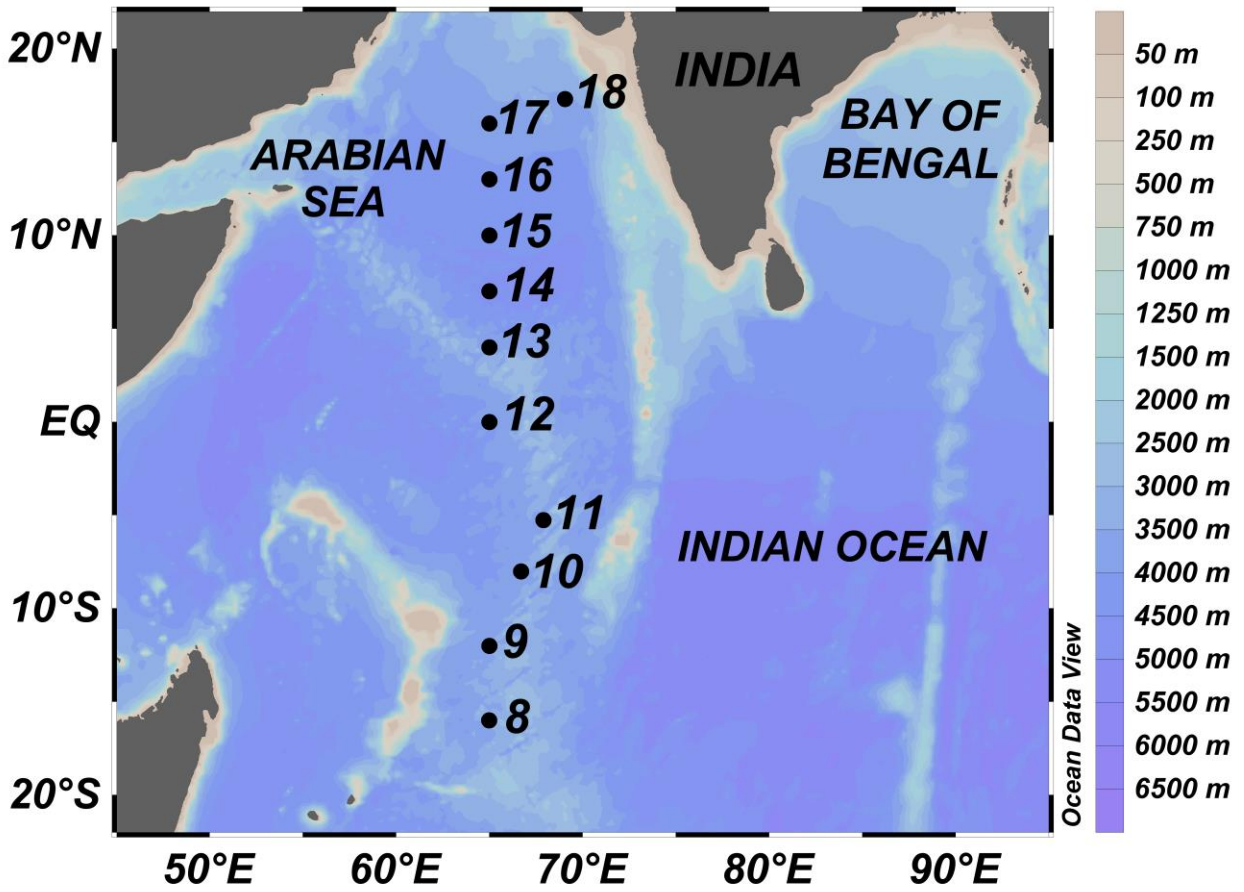


Figure 1.

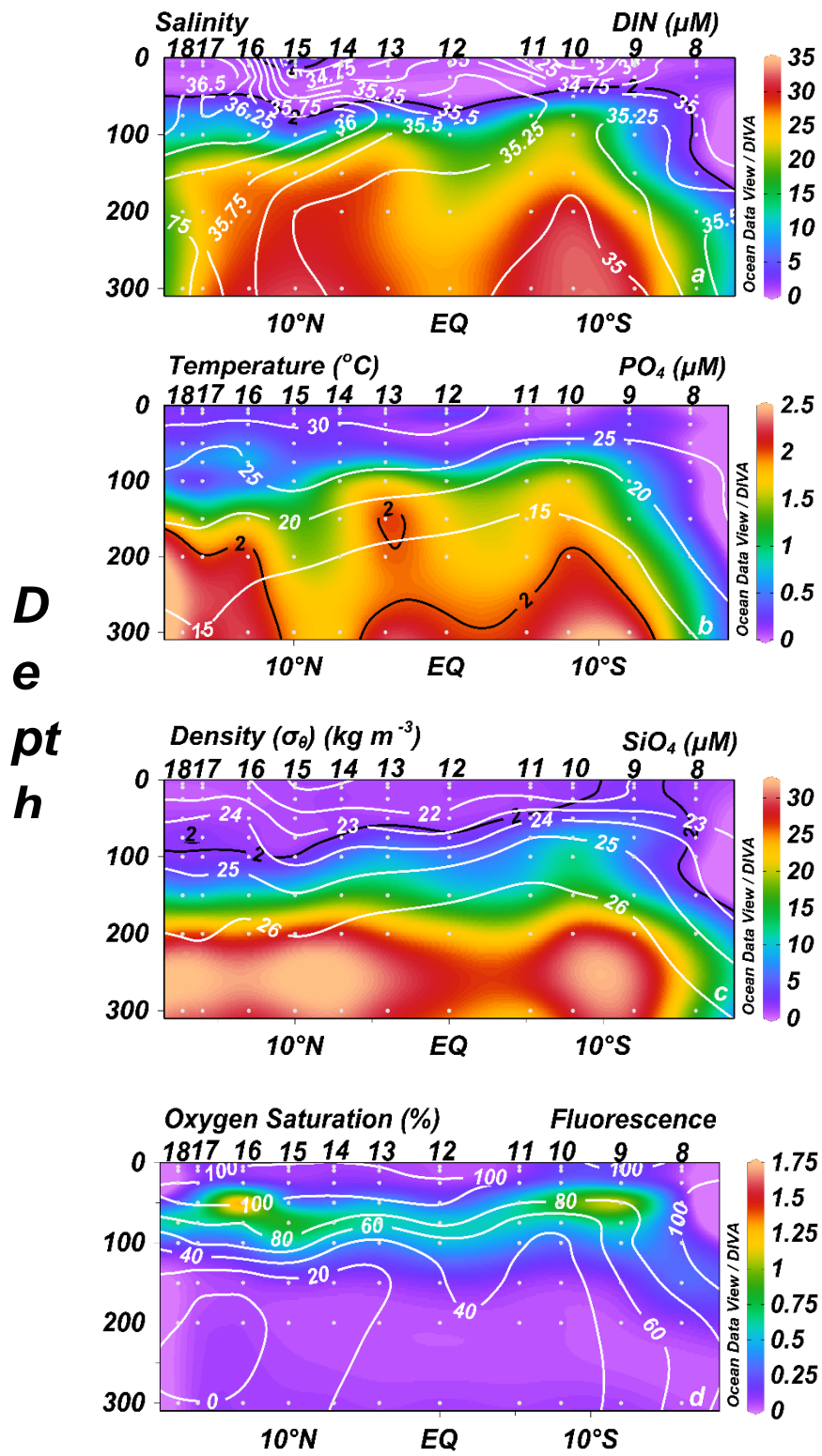


Figure. 2.

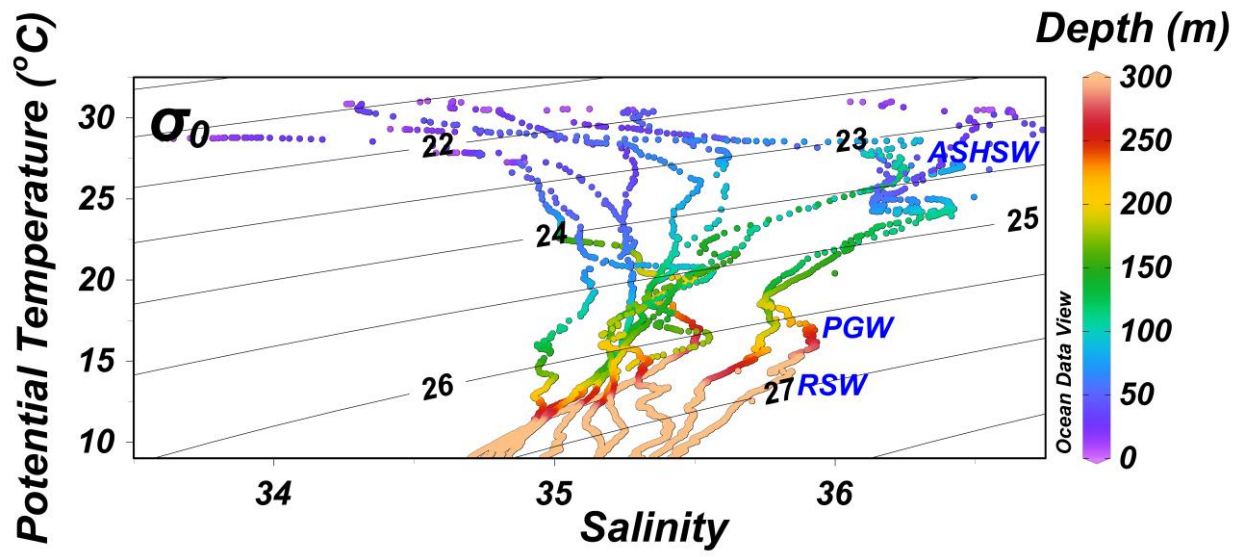


Figure 3.

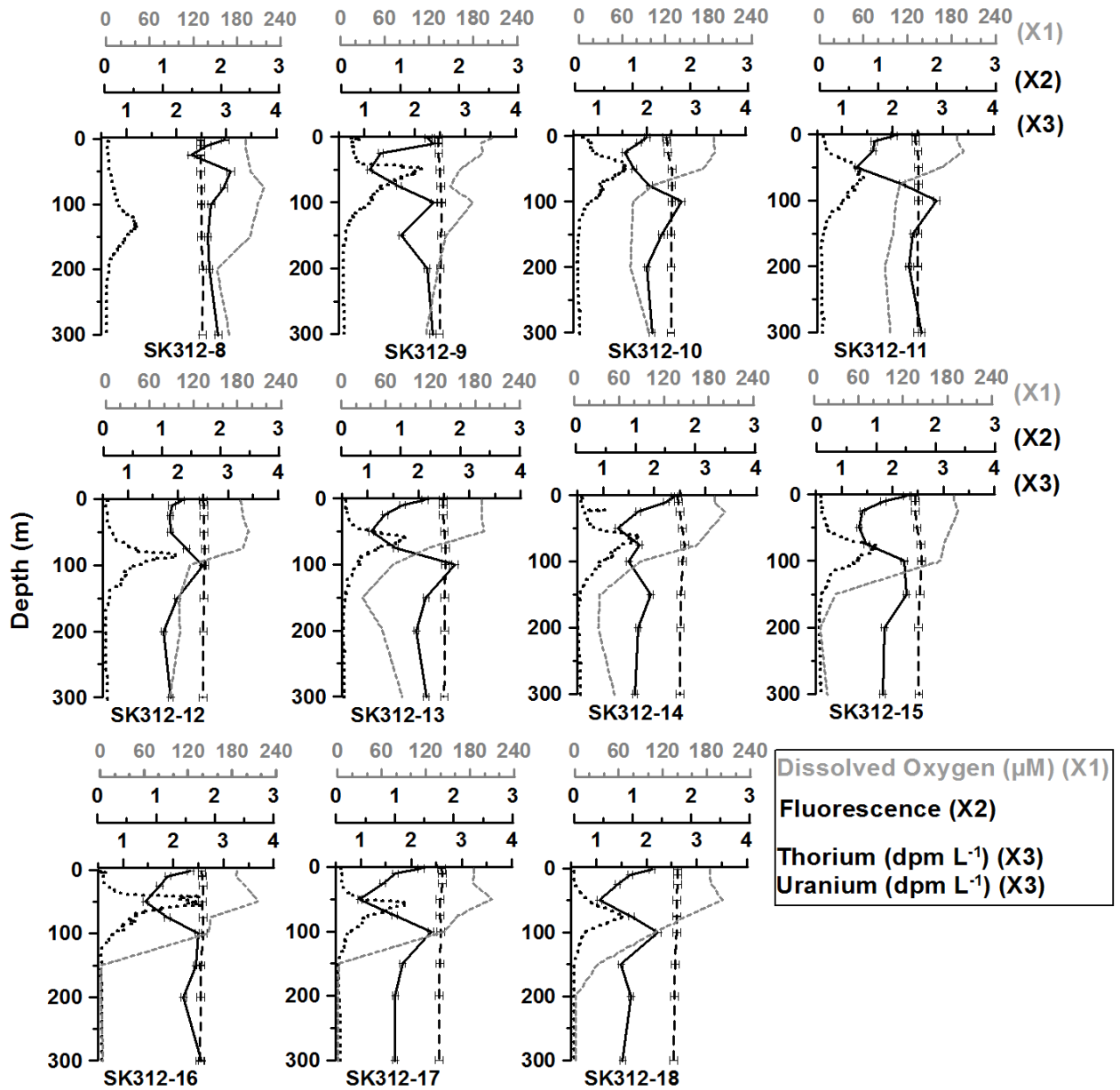


Figure 4.

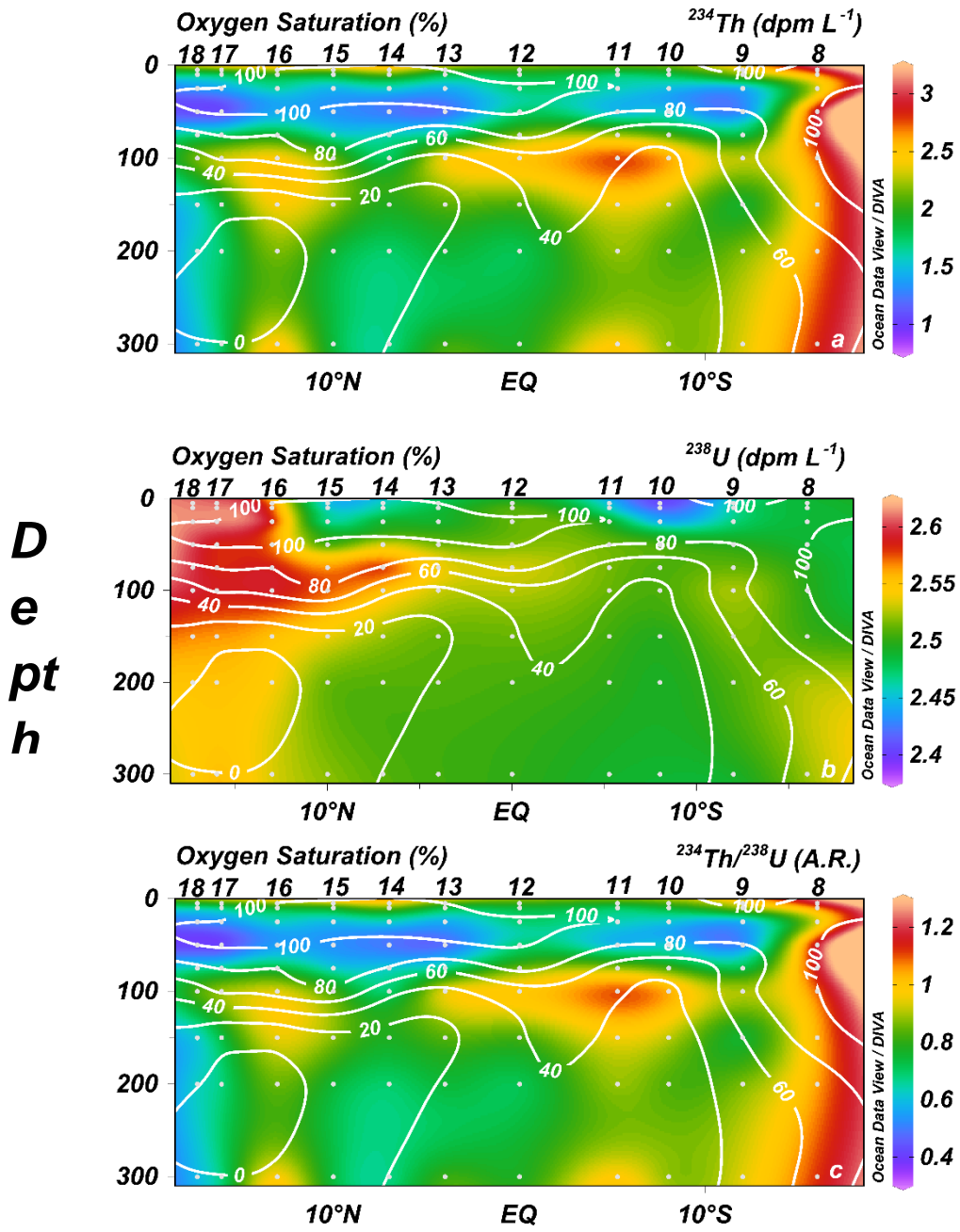


Figure 5.

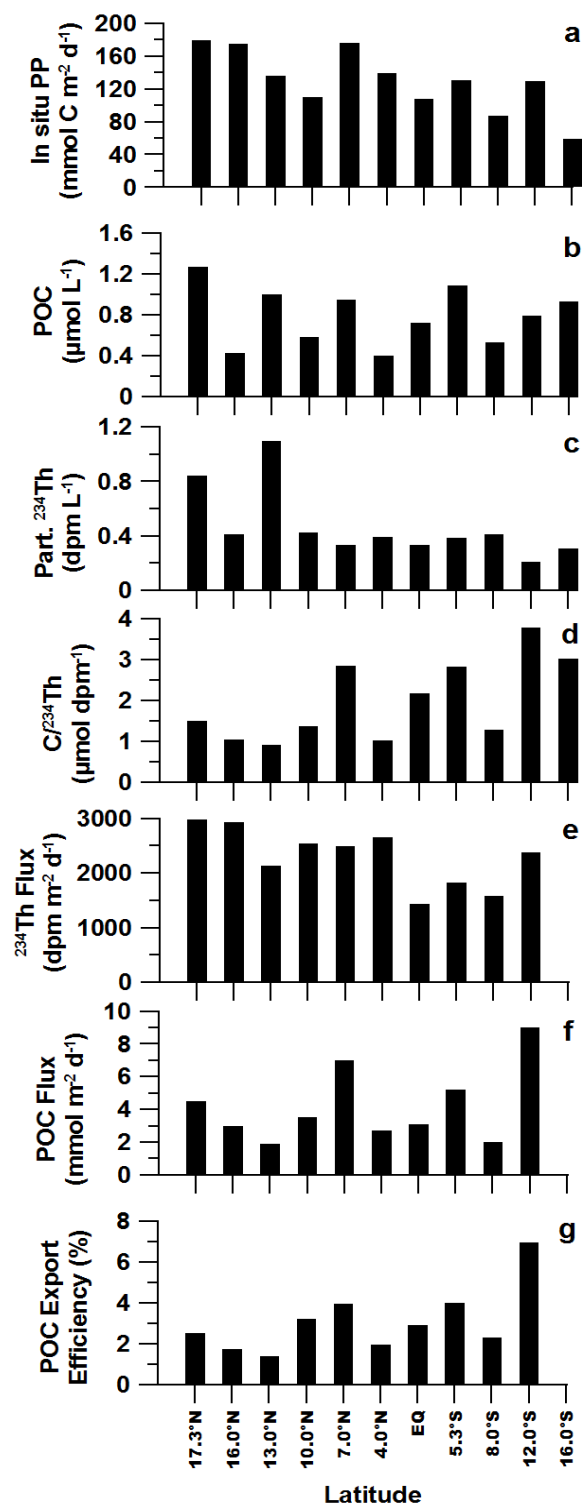


Figure 6.

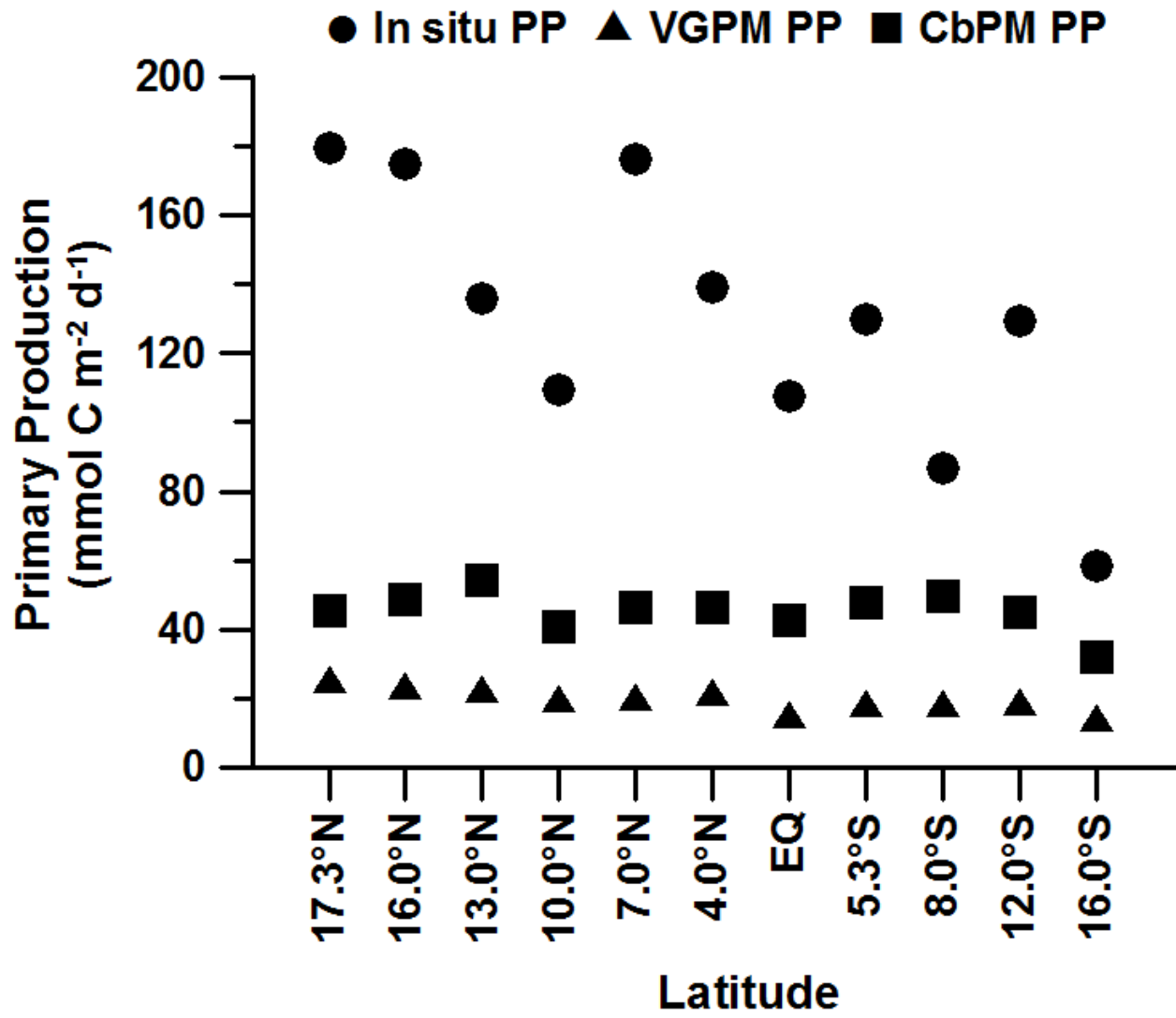


Figure 7

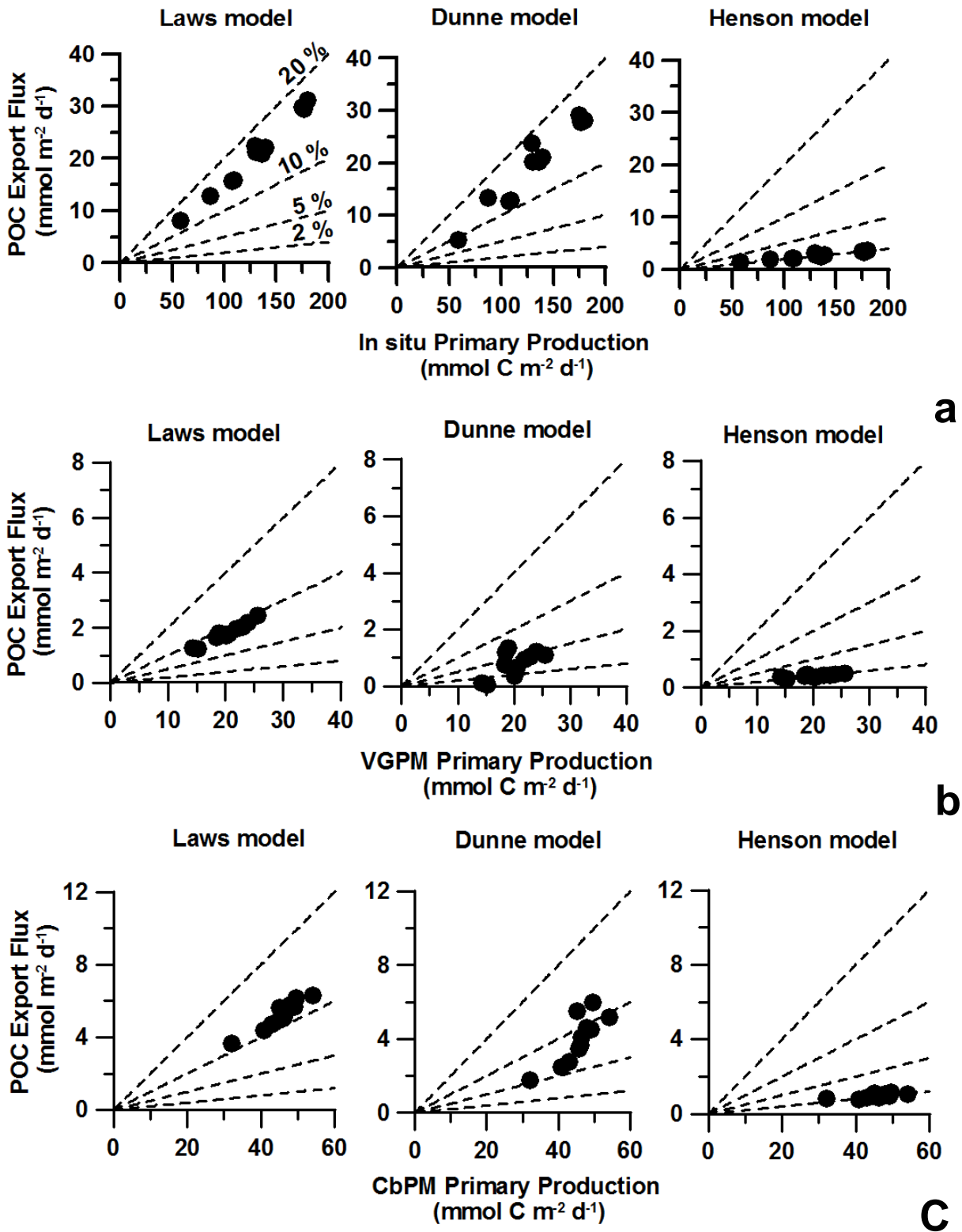


Figure 8

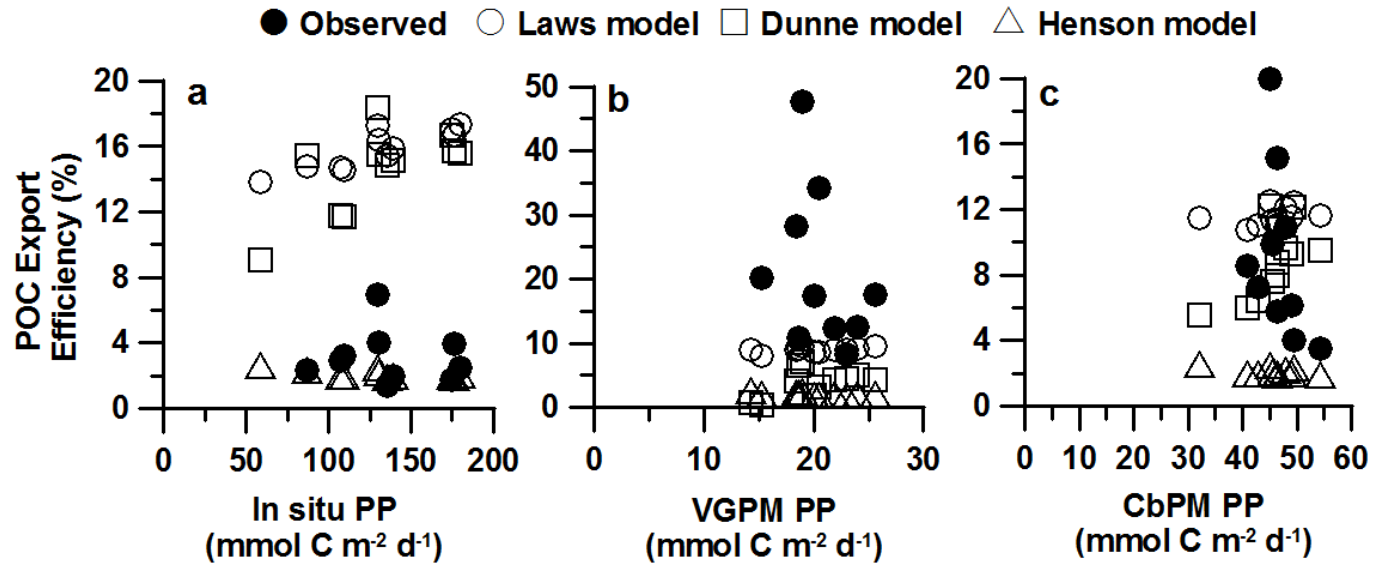


Figure 9